PROPERTIES OF LIGHT EMITTING DIODES FOLLOWING COBALT-60 IRRADIATION

A THESIS SUBMITTED TO
THE GRADUATE SCHOOL OF NATURAL AND APPLIED SCIENCES
OF
MIDDLE EAST TECHNICAL UNIVERSITY

BY

ŞAFAK ÖZCAN

IN PARTIAL FULFILLMENT OF THE REQUIREMENTS
FOR
THE DEGREE OF MASTER OF SCIENCE
IN
PHYSICS

SEPTEMBER 2004

Approval of the Graduate School of Natural and Applied Sciences

_____

Prof. Dr. Canan Özgen
Director

I certify that this thesis satisfies all the requirements as a thesis for the degree of Master of Science.

_____

Prof. Dr. Sinan Bilikmen
Head of Department

This is to certify that we have read this thesis and that in our opinion it is fully adequate, in scope and quality, as a thesis for the degree of Master of Science.

_____

Prof. Dr. İbrahim Günal
Supervisor

Examining Committee Members

Prof. Dr. Ay Melek Özer	(METU, PHYS)	_____
Prof. Dr. İbrahim Günal	(METU, PHYS)	_____
Assoc. Prof. Dr. Akif Esendemir	(METU, PHYS)	_____
Assoc. Prof. Dr. Mehmet Parlak	(METU, PHYS)	_____
Dr. Ali Alaçakır	(ANAEM)	_____

I hereby declare that all information in this document has been obtained and presented in accordance with academic rules and ethical conduct. I also declare that, as required by these rules and conduct, I have fully cited and referenced all material and results that are not original to this work.

Şafak, Özcan :

Signature :

ABSTRACT

PROPERTIES OF LIGHT EMITTING DIODES FOLLOWING COBALT-60 IRRADIATION

Özcan, Şafak
M.S., Department of Physics
Supervisor: Prof. Dr. İbrahim Günal

September 2004, 71 pages

The main purpose of this study is to investigate the effects of gamma radiation on the properties of the light emitting diodes. GaP and GaAsP LEDs are used in the study. It is observed that the exposure of a light emitting diode affects its various properties. A cobalt-60 gamma-cell is used to irradiate the selected light emitting diodes. For the different total doses of gamma pre-irradiation and post-irradiation I-V characteristics and spectral responses are recorded. The capacitance characteristics are measured at 1MHz at room temperature. Gamma ray bombardment of these LEDs results in reduction of electroluminescent intensity and increase in forward current up to levels tested. In GaP diodes dominant current transport mechanism has found to be effected by irradiation. No noticeable change is observed in the series resistances. The impurity density remains same in the green LED and increases in the red one due to the irradiation, which is deduced from the C-V characteristics. Both the circuit designers and the users should be aware of these effects in order to reach a reliable application for these components in a radiation environment.

Keywords: Light emitting diode, gamma radiation, cobalt-60, GaP, GaAsP, current transport mechanism, radiation damage

ÖZ

IŞIK SAÇAN DİYOTLARIN COBALT-60 RADYASYONU ALTINDAKİ ÖZELLİKLERİ

Özcan, Şafak
Y.Lisans, Fizik Bölümü
Tez Yöneticisi: Prof. Dr. İbrahim Günal

Eylül 2004, 71 sayfa

Bu çalışmanın asıl amacı gamma radyasyonunun ışık saçan diyotların (LED) özellikleri üzerindeki etkilerini araştırmaktır. Bu çalışmada GaP ve GaAsP ışık saçan diyotlar kullanılmıştır. Işınlamanın diyotların çeşitli özelliklerini değiştirdiği gözlemlenmiştir. Seçilen örnekler cobalt-60 gamma hücresi kullanılarak ışınlanmıştır. Çeşitli gamma dozları için ışınlama öncesi ve sonrası diyotların I-V karakteristikleri ve spektral dağılımları kaydedilmişir. Kapasitans ölçümleri 1MHz frekansta ve oda sıcaklığında yapılmıştır. Gamma ışınlaması bu LED'lerin elektriksel ışıldama şiddetinde azalmaya ve doğru yöndeki akımda artışa sebep olmaktadır. GaP diyotlarda baskın akım geçiş mekanizması radyasyonla değişmektedir. Seri dirençlerde gözlemlenebilir bir değişiklik olmamıştır. Işınlama sonucunda yeşil LED'lerde safsızlık atom yoğunluğu aynı kalmakta fakat kırmızı LED'lerde C-V ölçümlerinden görülebileceği üzere artmaktadır. Radyasyon etkisi altında bulunan ortamlarda kullanılacak bu tip LED'lerin devre tasarımcılarının ve kullanıcılarının güvenilir uygulamalar için bu cihazların özelliklerinin değişimlerini göz önünde bulundurmaları gerekmektedir.

Anahtar kelimeler: Işık saçan diyot, gamma ışıması, cobalt-60, GaP, GaAsP, akım geçiş mekanizması, radyasyon tahribatı

AKNOWLEDGMENTS

I would like to thank my thesis advisor Prof. Dr. İbrahim Günal for his guidance and support. I would like to acknowledge Dr. Ali Alaçakır for his collaboration in the exposure of Light Emitting Diodes and Assoc. Prof. Dr. Akif Esendemir for his help in the characterization of spectral responses of LEDs. Discussions with Prof. Dr. Raşit Turan about the experimental details are gratefully acknowledged.

TABLE OF CONTENTS

LIST OF TABLES

TABLE

LIST OF FIGURES

FIGURES

LIST OF SYMBOLS

(LED) Light Emitting Diode

(β) the beta particle

(γ) photon

(σ) cross section

(I) beam of intensity

(Φ) flux of photons per unit time and unit area

(N) density of atoms

(μ) total absorption coefficient

(ρ) material density

(N_a) Avogadro's number

(A) atomic mass

(ω_i) weight fraction of element i

($I(x)$) intensity of the beam after a distance x

(I_0) initial intensity

(D) total absorbed dose

(μ_{en}) energy absorption constant

(n_0 , p_0) thermal equilibrium electron and hole densities

(N_A, N_D) ionized acceptor and donor densities

(n_i) intrinsic carrier concentration

(ε_f) Fermi energy

($\varepsilon_c, \varepsilon_v$) lower limit of the conduction band and lower limit of the valance band

(K_s) relative dielectric constant

($\rho(x)$) charge density

(ρ) resistivity

(J) current density

(v_d) drift velocity

(μ) mobility

(D) diffusion constant

(V_{bi}) built in potential

(G_n, G_p) electron and hole generation rates

(U_n, U_p) recombination rates

(n_p) minority carrier density

(τ_n) electron lifetime

(L_p) diffusion length

(N_t) trap density

(V_{th}) carrier thermal velocity

(n) ideality factor

(a) grading constant

(C_j) junction capacitance

(R_s) series resistance

CHAPTER 1

INTRODUCTION

Design and operation of reliable systems in space environments require systems engineering approach. Light Emitting Diodes (LEDs) have many special application areas in space. LEDs are extremely sensitive to displacement damage effects. Radiation in space can cause permanent damage in LEDs that can lead to operational failure. Two application areas of light emitting diodes in space can be summarized as given below.

Astronauts in deep space are subjected to increased levels of radiation compared to low-earth orbit environments. Light Emitting Diode(LED) technology developed for NASA plant growth experiments in space shows promise for delivering light deep into tissues of the body to promote wound healing and human tissue growth .Studies on cell exposed to micro cavity and hyper gravity indicate that human cells need gravity to simulate growth. As the gravitational force increases or decreases, the cell function responds in a linear fashion. This causes significant health risks for astronauts in long-term space flight. The application of light therapy with the use of NASA LEDs will significantly improve the medical care that is available to astronauts on long-term space mission. NASA LEDs stimulate the basic energy processes in the mitochondria (energy compartments) of each cell, particularly when near-infrared light is used to activate the color sensitive chemicals inside.

Galileo's magnetic recorder was attributed to LED degradation. The encoder wheel position is detected by three LED-phototransistor pairs. If any of the phototransistors does not detect its LED's illumination when a window in the encoder wheel is in position, then the sequence would stop and the motor would draw either a high current or no current-high current and no motion are exactly the symptoms initially observed. Radiation could cause this by causing (a) a drop in LED light output, (b) a drop in the phototransistor's gain, or (c) darkening of the elements in the optical path

i.e. the LED and phototransistor lenses and/or the glass wheel.
In this thesis, ionizing radiation effects using cobalt-60 gamma rays were considered, to the exclusion of other radiation effects on electronics. This is because all radiation effects can be divided into ionizing and non-ionizing effects. Hence, it is possible to study the effects of total ionizing dose in isolation from non-ionizing effects. A gamma-ray source was used because other sources of radiation, such as proton or heavy ion beams, would cause non-ionizing radiation effects as well as ionizing radiation effects. The cobalt-60 source used was also readily available and inexpensive to operate, since no power needed to be supplied to the source for it to irradiate the devices under test. Its main disadvantage was its low dose rate. Electron or positron beams and X-ray sources would also be good sources of ionizing radiation without non-ionizing radiation effects, but they were not available for these tests. They would also be more expensive to operate than a cobalt-60 source.

The organization of the thesis is as follows:
Chapter 2 introduces brief information about light sources in markets today, light emitting diodes, working principle of LEDs and also the application areas.

Chapter 3 categorizes the radiation according to the effects and than specializes through the source used in this study and describes the interaction mechanism of this type of source with matter.

Chapter 4 includes the introduction to semiconductor physics basically. The following sections are focused on junction statistics and radiation damage effects on junction properties discussed previously.

Chapter 5 presents the experimental work done and gives the results with associating errors.

Chapter 6 includes analyze of the experimental results and explains the changes upon irradiation with the results of affect mechanisms.

Finally, Chapter 7 summarizes the results and conclusions of this study.

CHAPTER 2

LIGHT SOURCES IN ELECTRONICS

In this chapter after brief information of light sources in markets today, LED device structure, characteristics and application areas are discussed.Light can be produced and/or controlled electronically in a number of ways. In light emitting diodes (LEDs), light is produced by a solid state process called electroluminescence.

Under specific conditions, solid state light sources can produce coherent light, as in laser diodes. Other devices such as liquid crystal devices (LCDs) control externally supplied light to form display units. Liquid crystal projectors have made a major impact on public presentation of information, making inroads on the venerable cathode ray tubes. Other technologies such as the Texas Instruments' micromirror devices, called "digital light processors" as well as varieties of plasma displays are beginning to enter the market for displays.

Nowadays LED lighting is making great strides in power and efficiency and will play a more major role in general lighting. Some types last 100,000 hours, compared to about 1000 hours for an incandescent bulb. Now that blue LEDs have become a reality, white light LEDs can be produced by combining the red, green and blue chips in a single device.

The efficiency of a device in converting electrical power to visible light is called "luminous performance" in Figure 1, and is measured in lumens/watt. Low pressure sodium lights have very high efficiency because of the dominance of the sodium d-lines in the response of sodium vapor. As a tribute to the progress which has been made with LEDs, one type of red LED, the inverted pyramid type developed by Hewlett-Packard has exceeded the efficiency of "old yellow", the sodium light.

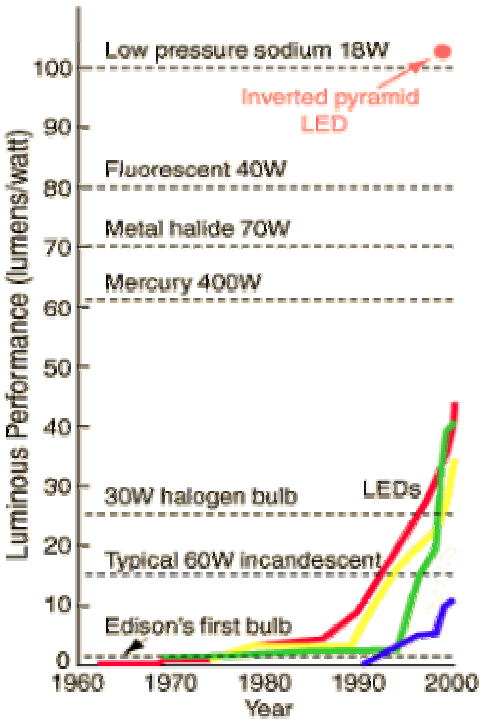

Figure 1. Luminous performance of devices in converting electrical power to visible light

2.1. Light Emitting Diodes (LEDs)

LEDs are solid-state semiconductor devices that convert electrical energy directly into light. Thermal sources of light such as flames and incandescent filaments emit light when heated, either by chemical reaction (flames) or electrical heating (filament lamps). LED "cold" generation of light leads to high efficacy because most of the energy radiates within the visible spectrum.

Other common high efficiency light sources, such as fluorescent lamps and electroluminescent devices, also produce light without much thermal radiation outside the visible spectrum. Because LEDs are the solid-state devices, they can be extremely small and durable; they also provide longer lamp life than other sources.

A LED is a special type of semiconductor diode. Like a normal diode, it consists of a chip of semiconducting material impregnated, or doped, with impurities to create a structure called a pn junction. Charge-carriers (electrons and holes) are created by an electric current passing through the junction, and release energy in the form of

photons as they recombine. The wavelength of the light, and therefore its color, depends on the band gap energy of the materials forming the pn junction. A normal diode, typically made of silicon or germanium, emits invisible far-infrared light, but the materials used for a LED have band gap energies corresponding to near-infrared, visible or near-ultraviolet light. Conventional LEDs are made of inorganic minerals such as:

- aluminium gallium arsenide (AlGaAs) - red and infrared
- gallium arsenide/phosphide (GaAsP) - red, orange and yellow
- gallium nitride (GaN) - green
- gallium phosphide (GaP) - green
- zinc selenide (ZnSe) - blue
- indium gallium nitride (InGaN) - blue
- silicon carbide (SiC) - blue
- diamond (C) - ultraviolet
- silicon (Si) - under development

LED development began with infrared and red devices, and technological advances have made possible the production of devices with ever shorter wavelengths.

Blue LEDs became available in the late 1990s. They can be added to existing red and green LEDs to produce white light. Most "white" LEDs in production today use a blue LED chip covered by a scintillator coating made of Zinc selenide (ZnSe). The LED chip emits blue light, part of which is converted to yellow by the ZnSe. This mixture of blue and yellow light creates the impression of white - hence the bluish or yellowish tint that these diodes usually exhibit.

The most recent innovation in LED technology is a device that can emit ultraviolet light. When ultraviolet light illuminates certain materials, these materials will fluoresce or give off visible light. White light LEDs have been produced by building ultraviolet elements inside material that fluoresces to produce white light.

Ultraviolet and blue LEDs are relatively expensive compared to the more common reds, greens, yellows and infrareds and are thus less commonly used in commercial

applications.

Most typical LEDs are designed to operate with no more than 30-60 miliwatts of electrical power. Around 1999, commercial LEDs capable of continuous use at one watt of input power were introduced. These LEDs used much larger semiconductor die sizes to handle the large power input. As well, the semiconductor die were mounted to metal slugs to allow for heat removal from the LED die.

In 2002, 5 watt LEDs were available with efficiencies of 18-22 lumens per watt. It is projected that by 2005, 10 watt units will be available with efficiencies of 60 lumens per watt. These devices will produce about as much light as a common 50 watt incandescent bulb, and will facilitate use of LEDs for general illumination needs.

In the last few years (up to 2003) there has been much research into organic LEDs or OLEDs, which are made of semiconducting organic polymers. The best efficiency of an OLED so far is about 10%. These promise to be much cheaper to fabricate than inorganic LEDs, and large arrays of them can be deposited on a screen using simple printing methods to create a color graphic display.

2.1.1. LED Device Structure

One way to construct a LED is to deposit three semiconductor layers on a substrate. Between p-type and n-type semiconductor layers, an active region emits light when an electron and hole recombine.

Considering the p-n combination to be a diode, then when the diode is forward biased, holes from the p-type material and electrons from the n-type material are both driven into the active region. The light is produced by a solid state process called electroluminescence.

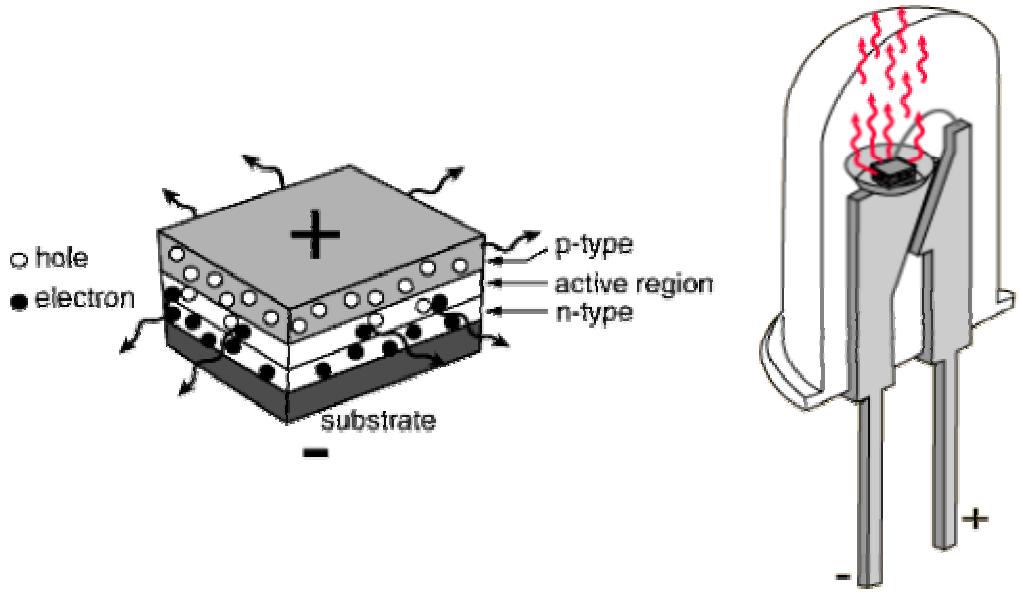

(a) (b)

Figure 2. Schematic diagram of a LED (a) Layers of a LED; (b) LED structure

In this particular design, the layers of the LED emit light all the way around the layered structure, and the LED structure is placed in a tiny reflective cup so that the light from the active layer will be reflected toward the desired exit direction. The reflective cup may be colored, but this is only for cosmetic reasons and does not affect the color of the light emitted. Schematic representation for a LED is illustrated in Figure 2.

2.1.2. LED Characteristics

LEDs require a DC supply of the correct polarity. When the voltage across the pn junction is in the correct direction, a significant current flows and the device is said to be forward biased. The voltage across the LED in this case is fixed for a given LED and is proportional to the energy of the emitted photons. If the voltage is of the wrong polarity, the device is said to be reverse biased at which very little current flows, and no light is emitted.

When an LED is forward biased to the threshold of conduction, its current increases rapidly and must be controlled to prevent destruction of the device. The light output is quite linearly proportional to the current within its active region, so the

light output can be precisely modulated to send an undistorted signal through a fiber optic cable. The light output versus forward current is given by Figure 3.

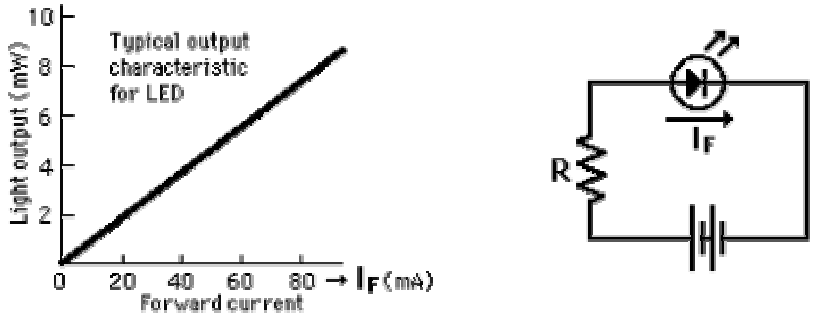

Figure 3. Light output versus forward current characteristics

2.1.3. LED Applications

LEDs offer benefits in terms of maintenance and safety. The typical working lifetime of a device, including the bulb, is ten years, which is much longer than the lifetimes of most other light sources. LEDs give off less heat than incandescent light bulbs and are less fragile than fluorescent lamps. Since an individual device is smaller than a centimeter in length, LED-based light sources used for illumination and outdoor signals are built using clusters of tens of devices. Incandescent light bulbs for traffic signals and pedestrian crosswalks are gradually being replaced by LED clusters. Lighting systems using incandescent bulbs are cheap to buy but inefficient. However, fluorescent tubes are more efficient, but are bulky and fragile and require starter circuits. In addition to the most specialized application areas of LEDs, other applications are given below:

- thin, lightweight message displays (e.g. in public information signs)
- status indicators (e.g. on/off lights)
- Bicycle lighting.
- illumination (e.g. flashlights [a.k.a. torches, U.K.], backlights for LCD displays)
- signaling/emergency beacons and strobes

- infrared remote controllers
- sensors (e.g. mechanical and optical mice)
- LED printers

LEDs are robust and moderately efficient, up to 32 lumen per watt, but are expensive, although their cost is falling. The technologies for LED production are developing rapidly to improve the properties. The high brightness LEDs are good example for these improvements.

High brightness LEDs (HBLEDs) offer much higher performance than traditional LEDs, but come with significantly higher cost. The demand for high brightness LEDs is growing rapidly because of their high efficiency, long life, and wide range of available colors. These characteristics are driving their use in applications in stead of traditional LEDs.

CHAPTER 3

RADIATION SOURCES

In this chapter the radiation is categorized according to the effect mechanism. In the following parts the source used in this study is explained and also the effect of this type of radiation through material is discussed.

3.1. Types of Radiation

All radiation can be divided into two main categories - non-ionizing radiation and ionizing radiation. Charged hadrons and leptons, heavy ions, and photons are considered ionizing radiation, as they can ionize an atom through electromagnetic interactions. Neutrons and other neutral hadrons do not ionize atoms, and are therefore non-ionizing radiation.

Neutral particles, such as neutrons, interact with matter through non-ionizing energy loss mechanisms. In the case of neutrons with energy in the MeV range, the primary mechanism for energy loss is elastic scattering from atomic nuclei (Leo, 1994). This results in displacement of the atom in the lattice of the material.

For neutrons with sufficient energy to excite the nucleus, inelastic scattering may also occur. This leaves the nucleus in an excited state which may later decay by emitting gamma rays or other radiation. Low energy neutrons with energy in the eV to keV range may undergo nuclear reactions such as radiative neutron capture (Leo, 1994). This may also result in an unstable nucleus, which will alpha or beta decay. Although the neutrons themselves do not ionize atoms, they may produce unstable nuclei which will produce ionizing radiation.

Gamma rays and other high-energy photons interact with matter in three ways: the photo-electric effect, the Compton effect, and pair production (Evans,1955; Leo, 1994). The interaction of gamma rays with matter is more fully described in section

3.2. The photo-electric and Compton effects result in the ejection of energetic electrons and the ionization of atoms. Pair production produces electron-positron pairs. The energetic electrons and positrons from these three processes are responsible for most of the ionization of the material.

Charged particles can also ionize atoms. For the purposes of radiation effects, charged particles can be divided into light particles (electrons and positrons) and heavy particles (muons, hadrons, and nuclei) (Leo, 1994). These charged particles will lose their energy through inelastic collisions with atomic electrons and elastic scattering from nuclei. Heavy charged particles lose most of their energy through inelastic collisions with electrons (Leo, 1994). These collisions will excite the atomic electrons. Ionization results if enough energy is transferred, from the heavy particle to the electrons in the collisions. The recoil electrons may also have enough energy to cause secondary ionization. The effects of elastic scattering of heavy charged particles from nuclei is similar to the effects of neutrons colliding with nuclei, resulting in atomic displacements.

Electrons and positrons also lose energy from collisions with atomic electrons in much the same way as heavier particles. Since they have a much smaller mass, however, they are also subject to energy losses from bremsstrahlung (electromagnetic radiation emitted by the electron as it is loses energy through interaction with the electric field of an atomic nucleus). Bremsstrahlung is a minor factor for electrons with energies below a few MeV, but dominates energy loss from collisions for electrons with energies of a few tens of MeV (Leo, 1994). Through colliding with atomic electrons, free electrons will ionize more atoms until they lose enough energy from collisions that they fall below the ionization threshold energy. In the meantime, secondary electrons from previous collisions or bremsstrahlung photons will cause secondary ionization.

3.2. Cobalt-60 Sources

One of the standard gamma-ray sources used in radiation testing of electronic devices is cobalt-60. Cobalt-60 is an unstable isotope with 27 protons and 33 neutrons, which beta-decays into nickel-60. The energy level diagram for this decay

is shown in Figure 4. The beta particle (β) emitted has a maximum energy of 0.314 MeV, and an average energy of 0.093 MeV. The half-life of this decay is 5.27 years (Spinks and Woods, 1964). The resulting nickel nucleus is usually in an excited state, which quickly decays into a stable state by emitting a 1.173 MeV photon (γ), followed by a 1.332 MeV photon. For many purposes, mean gamma energy of 1.25 MeV is used in calculations. Less that one in 10^6 cobalt-60 nuclei beta decay directly into the ground state of nickel-60 (Evans, 1955).

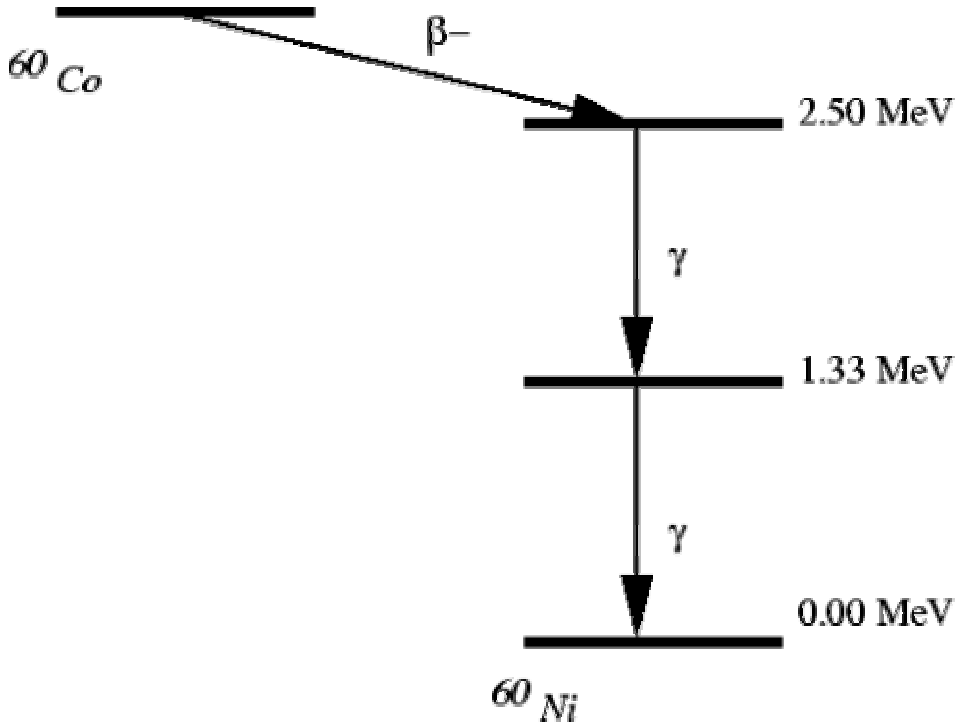

Figure 4. Dominant decay scheme of cobalt-60

Nickel-60 is a stable isotope, so a pure cobalt-60 source will not produce any radiation other than those from cobalt-60 beta and gamma decay. However, the interaction of the beta and gamma particles produced by cobalt-60 with the environment through Compton scattering and pair production will produce a spectrum of particles (Woolf and Frederickson,1983).

There are two main types of cobalt-60 sources: cavity-type sources and cave-type sources. In cavity sources, the cobalt-60 irradiates a cavity surrounded by shielding material (usually lead). Samples to be irradiated are placed inside the cavity. Movable shielding is used so that the sample can be introduced without exposing the cobalt-60.

In a cave source, the shielding is immobile, but the source is movable. In cave sources, the cobalt-60 is kept in a shielded container. The sample to be irradiated is placed in a small room, or cave, and the source is moved out of its container and into the cave. Since the source is exposed unshielded in the cave, the cave must also be shielded from the outside environment, usually with concrete walls. The cave's entrance is also isolated from the radiation area by building the cave in the form of a labyrinth.

3.3. Interaction of Gamma Rays with Matter

Photons in the keV to MeV range produced by the de-excitation of nuclei are referred to as gamma rays. Photons produced by atomic de-excitation, with energies in the eV to keV ranges, are referred to as X-rays. These photons interact with matter in three ways: photo-electric effect (the primary means of interaction for low-energy X-rays), the Compton effect (which is more important for high-energy photons), and pair production (which is only possible for photons with energy greater than 1.022 MeV, or twice the mass of the electron (Evans, 1955; Leo, 1994).

In the photoelectric effect, a photon is completely absorbed by an atomic electron, which is then ejected from the atom with energy equal to the photon's energy minus the binding energy of the electron. This must involve an atomic rather than a free electron, as the recoil of the nucleus is needed to take care of conservation of momentum.

In Compton scattering, a photon interacts with a free electron (or a bound electron, if the photon energy is much larger than the binding energy), resulting in an electron and photon of reduced energy scattered off at an angle. The energy of the scattered electron and photon depends on the scattering angle.

Pair production involves the production of an electron-positron pair from a photon. For momentum to be conserved, a third body, such as an atomic nucleus, is required. Cobalt-60 gamma rays of average energy 1.25 MeV are of sufficient energy for pair production to occur.

The total cross section per atom for a photon interacting with matter is thus

$$\sigma = \sigma_{photo} + \sigma_{Copm} + \sigma_{pair}\,, \tag{3.1}$$

σ_{Comp} can be expressed as the sum of two cross sections (Evans, 1955; Leo, 1994):

$$\sigma_{Comp} = \sigma^{a} + \sigma^{s}\,, \tag{3.2}$$

where σ^{a} is the Compton absorption cross-section, and σ^{s} is the Compton scattering cross-section. σ^{s}/σ_{Comp} is the average fraction of the original photon's energy $\overline{E}$ which is contained in the scattered photon, while σ^{a}/σ_{Comp} is the average fraction of E which is contained in the recoil electron.

For a photon beam of intensity I (in units of energy per unit time and unit area), where

$$I = \Phi E\,, \tag{3.3}$$

and Φ is the flux of photons per unit time and unit area, the flux of primary photons lost through the three photon interactions through a distance dx is

$$d\Phi = \Phi N\left(\sigma_{photo} + \sigma_{Comp} + \sigma_{pair}\right), \tag{3.4}$$

where N is the density of atoms. This translates to a loss in intensity of

$$dI = \Phi EN\left(\sigma_{photo} + \sigma_{Comp} + \sigma_{pair}\right) \tag{3.5}$$

where μ is the total absorption coefficient, defined as

$$\mu = N\sigma = \sigma\left(N_a \rho / A\right), \tag{3.6}$$

with ρ the material density, N_a Avogadro's number, and A the atomic mass (Leo, 1994). μ/ρ is the more commonly tabulated value, as this quantity is independent of the physical state of the substance. For chemical compounds or mixtures of materials, μ/ρ can be calculated using Bragg's rule,

$$\frac{\mu}{\rho} = \sum_{i=1}^{n} w_i \frac{\mu_i}{\rho_i}, \tag{3.7}$$

with ω_i being the weight fraction of element i in the compound or mixture (Evans,1955; Leo, 1994).

The attenuation of a beam of photons after passing through a thickness x of material then becomes (Evans, 1955; Leo, 1994)

$$I(x) = I_0 e^{-\mu x} = I_0 e^{(-\mu/\rho)\rho x}, \tag{3.8}$$

where $I(x)$ is the intensity of the beam after a distance x, and I_0 is the initial intensity.

In all three energy-loss mechanisms, the primary photons lose energy and produce secondary electrons (and positrons in the case of pair production). These electrons and positrons lose their energy primarily through collisions with atomic electrons (Leo, 1994).

Note that μ is the attenuation coefficient for absorption of primary photons only and Equation (3.8) gives the intensity of the beam of original photons only. It can be used to find the attenuation of the original beam of photons of energy E, neglecting all secondary particles. However, in Compton scattering, only a fraction of the primary photon's energy is transferred to the electron. As well, photons of lower energy than E can be scattered via multiple collisions back into the direction of the original beam.

When assessing radiation damage on electronic devices, the relevant quantity is the total absorbed dose D. D is defined as the total energy absorbed by a medium due to irradiation per unit mass. Thus, the relevant constant for the purposes of assessing the attenuation of the ionizing dose rate from a gamma ray source is not μ, but μ_{en}, the energy absorption constant.

To calculate μ_{en}, the relevant quantity is the energy transferred to the secondary electrons produced by the incident photons. In the photoelectric effect, this is simply E minus the binding energy of the electron E_b. For pair production, each electron-positron pair has a total energy of $E - 2m_e$. In the Compton Effect, the recoil electron has an average energy of $E(\sigma^a / \sigma_{Comp})$. Thus, Equation (3.5) is replaced by (Evans, 1955)

$$dI = \Phi N\left(\sigma_{photo}(E - E_b) + \sigma_{Comp}(E\frac{\sigma^a}{\sigma_{Comp}}) + \sigma_{pair}(E - 2m_e) \right)dx . \qquad (3.9)$$

In the approximation where E_b and m_e are neglected, this is simply (Evans, 1955)

$$dI = \Phi NE\left(\sigma_{photo} + \sigma^a + \sigma_{pair}\right)dx = I\mu_{en}dx . \qquad (3.10)$$

This leads to

$$I(x) = I_0 e^{-\mu_{en}x} = I_0 e^{(-\mu_{en}/\rho)}\rho x , \qquad (3.11)$$

For cobalt-60 gamma rays, the Compton Effect dominates, and the cross-sections for the photoelectric effect and pair production are comparatively low. In fact, the cross-section for pair production is negligible (Evans, 1955). Thus, even though $2m_e$ is not really negligible with respect to E, this exponential approximation can be used.

Dose is defined as the energy transferred to a medium due to ionization per unit mass. The usual units for dose are the Grey, which is defined as 1 J/kg, and the rad, which is equal to 100 erg/g or 0.01 Grey. The dose rate can be calculated from the

intensity of the photon beam using the simple relation (Evans, 1955)

$$\frac{dD}{dt} = I \frac{\mu_{en}}{\rho}. \tag{3.12}$$

Note that the dose rate from a gamma source of a given intensity varies according to the atomic composition and the density of the medium.

Since σ_{photo} is proportional to Z^n (where n is approximately 4.5) when E is in the MeV energy range, σ_{Comp} is roughly proportional to $\overline{Z}$, and σ_{pair} is proportional to Z^2 (Evans, 1955), the total interaction cross section, and thus the attenuation constant, increases for high Z materials. This is why dense materials with high atomic numbers, such as lead, are extensively used in radiation shielding.

There is one problem with the use of high Z materials as shielding, however: the existence of ``backscattered'' radiation. The low-energy secondary electrons produced by photon interaction are susceptible to scatter from atomic nuclei and will be deflected at large angles. The possibility of an electron being reflected from the surface of an absorber increases for high Z nuclei (Leo, 1994). As a result, if primary or secondary photons interact with the air inside an enclosure surrounded by a high Z material, backscattered electrons may be reflected into the cavity. Thus, the dose received at the centre (where dosimeters or electronics are undergoing tests) will be increased, and will not be purely the result of photons.

CHAPTER 4

JUNCTION STATISTICS AND DEFECTS UNDER RADIATION

In this chapter after an introduction to semiconductor physics, junction statistics of an ideal diode is discussed. In the following section forward bias deviations from the ideality are explained. At the end, the damages produced by gamma radiation and also the defects effecting the electrical properties of a junction described.

4.1. Introduction to semiconductor Physics

Electrons surrounding an atomic nucleus have certain well-defined energy levels. When numbers of atoms are grouped together, the energy levels fall into certain fixed bands made up of the discrete energy levels of individual electrons. Between the bands are empty band gaps in which no electrons are to be found. A band which is completely full or empty of electrons cannot conduct. An electron which is partaking in conduction is said to be in the conduction band, which lies immediately above the valance band.

At very low temperatures, the valance band for a semiconductor is full and the conduction band is empty, so that the semiconductor behaves like an insulator. As energy is applied, electrons move across the band gap from the valance band into the conduction band, leaving behind a hole which behaves like a positive charge carrier equal in magnitude to that of the electron. Both the conduction and valance bands can conduct (via electrons and holes), producing a bipolar (two-carrier) conductor. In order to make use of semiconductor, we need to be able to produce material which carries current either through electrons or through holes, but not both. This done by introducing impurities (usually called dopants) into the semiconductor lattice.

4.1.1. Extrinsic Carrier Densities

We would usually like higher carrier densities than can be obtained from intrinsic generation, and we would like $n >> p$ or $p >> n$ rather than $n = p$ obtained in the intrinsic case. This can be accomplished by doping the semiconductor. Doping simply means that atoms of different type are substituted for some of the host atoms in the crystal. Such a doped crystal is called extrinsic. For example, if V group atom such as Phosphorus is substituted for one of the silicon atoms, the phosphorus atom has five electrons in its outer shell, and after sharing four of these with silicon, the fifth electron has no covalent bond. The fact that group V atoms (P, As, and Sb) add extra electrons when substituted in to the lattice has resulted in their being termed donor atoms. The density of donor atoms are given by N_D. The energy levels of the donor impurities lie in the forbidden gap, usually very close to the edge of the conduction band. Hence, it takes very little energy to excite an electron from a donor atom into conduction band, and this leaves behind a positively ionized, immobile donor atom. It usually assumed that at room temperature all of the donors are ionized; hence we have N_D extra electrons in the conduction band in addition to those present due to intrinsic excitation. Similarly a group III (B, Al, Ga) atom substituted for as silicon atom, is called an acceptor impurity. The density of the acceptor impurities is termed by N_A. The group III atoms have three electrons in their outer shell to form covalent bonds with neighboring atoms, and one more electron is needed to complete the bonds. The energy level of the group II atoms lies very close to the valance band edge; consequently, it is very easy for the acceptor to capture an electron from the valance band and leave behind a hole near the top of the valance band. This also creates a negatively ionized immobile acceptor atom. The acceptor level is usually close enough to the valance band so that all of the acceptor atoms are ionized at room temperature; thus density of the holes is N_A plus the intrinsically excited holes. Gallium arsenide on the other hand, is doped differently. One can still make n-type or p-type material, but it can substituting group II, IV, or VI for the host atoms. The crystal must be electrically neutral;

$$n_0 + N_A = p_0 + N_D, \tag{4.1}$$

where n_0, p_0 are the thermal equilibrium electron and hole densities, respectively, and N_A and N_D are ionized acceptor and donor densities. For most cases either

$$N_D >> N_A, \quad N_D >> n_i, \qquad \text{n-type} \qquad (4.2)$$

n_i is the intrinsic carrier concentration,

or

$$N_A >> N_D, \quad N_A >> n_i. \qquad \text{p-type} \qquad (4.3)$$

For the conditions in Equation (4.2) donor density will be equal to;

$$n_{n0} \cong N_D = N_C \exp\left(\frac{\varepsilon_f - \varepsilon_c}{kT}\right). \qquad (4.4)$$

In particular,

$$p_{n0} = N_v \exp\left(\frac{\varepsilon_v - \varepsilon_f}{kT}\right), \qquad (4.5)$$

ε_f is the Fermi energy and ε_c and ε_v are lower limit of the conduction band and lower limit of the valance band respectively(Chaffin, 1973).

The make up of a simple semiconductor device, n-type substrate with a p-type layer implanted on it. When such a device is forward biased, current flows through the device. When the device is reverse biased, very little current flows (at least until the device breakdown voltage is reached).

4.1.2. Junction Statistics

In this part we focus our attention on the transition region between the p nd n

regions of the diode under static biasing conditions, examining, in turn, thermal equilibrium($V_A = 0$), forward bias($V_A > 0$). The region near the metallurgical junction, the transition region, is often called the depletion region since the mobile carriers in the region are reduced in number that is, depleted in population compared to the bulk regions far from the junction. We first consider the junction under equilibrium conditions qualitatively to establish the source of the charge density, electric field, and potential in the depletion region. With these quantities established, the concept of the built in potential (V_{bi}) is introduced and treated quantitatively. The depletion approximation is next invoked to solve Poisson's Equation for $E(x)$ and $V(x)$, assuming a step junction profile and $V_A = 0$.

4.1.3. Qualitative Equilibrium Electrostatics

Before discussing the static properties of the junction, let us clearly specify the assumptions. The entire list of assumptions includes

1. a one dimensional device
2. a metallurgical junction at x=0
3. a step junction from N_A to N_D with uniformly doped p and n regions
4. perfect ohmic contacts far removed from metallurgical junction.

In the step junction diode, sections of the semiconductor are uniformly doped, but the doping is different on the opposite sides of the metallurgical junction.

In our particular case 'equilibrium' means no applied voltage $V_A = 0$, no light shinning on the device, no thermal gradients (uniform temperature) and no applied magnetic and electric fields. The situation external to the device is clearly little of interest. The internal situation, on the other hand is quite interesting. I attempt to ascertain the internal situation, first assume charge neutrality exists everywhere in the device. The holes would therefore expect to diffuse so as to make their numbers more homogeneous throughout the material. Similar arguments hold for the electrons. This assumption indicates that the holes will diffuse from the p side to n side and electrons will flow fro n side to p side. Ideally the diffusion process will

continue until the carrier concentrations become equal on both sides of the junction. The diffusion process however can not continue forever because it disturbs the charge balance between $-qN_A$ and qp_p on the p side of the junction and between qN_D and $-qn_n$ on the n side of the junction. When the holes diffuse away fro the p side, they leave behind the ionized acceptor atoms (N_A) that are fixed in place within the crystal lattice. On the n side electrons diffuse away, leaving the ionized donor atoms (N_D). Obviously a net charge density similar to Equation (4.1) must be created by the reduction of majority carrier concentrations. From the Gauss's law, a net charge density implies in turn the existence of an electric field and therefore a potential difference. The electric field thus opposes diffusion of holes from the p side and electrons from the n side.

The general form of the electric field can be established through the use of equation given below, where the charge density is equal to the imbalance between the charge carriers and the ions.

$$E(X) = \frac{1}{K_s \varepsilon_0} \int_{-\infty}^{x} \rho(x) dx \,, \tag{4.6}$$

where K_s the relative dielectric constant of the semiconductor and the charge density is $\rho(x)$ is given by $p - n + N_D - N_A$.

The charged region near the metallurgical junction where the mobile carriers have been reduced is called the depletion region. With a charge density and resultant electric field present within the structure, there must also be a potential gradient. From electromagnetic field theory,

$$E = -\nabla V(x) \,. \tag{4.7}$$

4.1.4. Built In Potential

A voltage called the built in potential, exists across the depletion region of the device even at thermal equilibrium. The built in potential can be thought of as similar to the

contact potential between to dissimilar metals.

There are two ways in which current can flow: drift in an electric field and diffusion due to a concentration gradient. At low electric field the drift velocity (v_d) is proportional to the electric field strength (E), and the proportionality constant is defined as the mobility, or

$$v_d = \mu E . \tag{4.8}$$

Its reciprocal value is conductivity. Since the resistivity (ρ) is defined as the proportionality constant between the electric field and the current density (J):

$$J = \sigma E . \tag{4.9}$$

For semiconductors both electrons and holes are carriers, we obtain

$$\rho = \frac{1}{\sigma} = \frac{1}{q(\mu_n n + \mu_p p)} . \tag{4.10}$$

By combining Equations (4.7) and (4.8) drift current density due to electric field can be written as

$$J_{drift} = q(\mu_n n + \mu_p p)E . \tag{4.11}$$

The diffusion current density due to concentration gradient for electrons and holes respectively is given by ;

$$J_{ndiffusion} = +qD_n \nabla n , \tag{4.12}$$

and

$$J_{pdiffusion} = -qD_p \nabla p . \tag{4.13}$$

As Equation (4.9) contains drift currents of electrons and holes current density equations for electrons and holes can be written as;

$$J_{n,p} = q\mu_{n,p} n, pE \mp qD_{n,p} \frac{dn, p}{dx}, \tag{4.14}$$

and the total current density is given by

$$J = J_n + J_p . \tag{4.15}$$

For thermal equilibrium $(V_A = 0)$ $J = J_n = J_p = 0$. A glance at Equation (4.12) quickly reveals the need for

$$J_{ndrift} = -J_{ndiffusion}, \tag{4.16}$$

and similarly

$$J_{pdrift} = -J_{pdiffusion} . \tag{4.17}$$

Consequently, the zero net current density for each carrier type under equilibrium conditions is achieved through a cancellation of the drift component by an oppositely directed diffusion component of equal magnitude.

By using Equations (4.14) and (4.16) and solving for the electric field yields,

$$E = \left(\frac{-qD_n}{q\mu_n n} \right) \left(\frac{dn}{dx} \right). \tag{4.18}$$

By using the Einstein relationship Equation (4.18) reduces to,

$$E = -\left(\frac{kT}{q} \right) \left(\frac{1}{n} \right) \left(\frac{dn}{dx} \right). \tag{4.19}$$

Using Equation (4.7) and Equation (4.19), the voltage across the ends of the p-n junction can be written as;

$$V_{bi} = \frac{kT}{q} \int_{-\infty}^{+\infty} \left(\frac{1}{n} \right) \left(\frac{dn}{dx} \right) dx = \frac{kT}{q} \int_{n(-\infty)}^{n(+\infty)} \frac{dn}{n}, \tag{4.20}$$

integrating we obtain

$$V_{bi} = \frac{kT}{q} \ln n \Big|_{n(-\infty)}^{n(+\infty)}. \tag{4.21}$$

To define boundary conditions of Equation (4.21), intrinsic carrier concentration can be obtained from Equation (4.4) and Equation (4.5) and using the fact that

$$n_{n0} p_{n0} = n_{p0} p_{p0} = n_i^2 . \tag{4.22}$$

We can combine Equation (4.1) and Equation (4.22) to give the concentration of electrons and holes in an n-type semiconductor:

$$n_{n0} = \frac{1}{2}\left[\left(N_D - N_A\right) + \sqrt{(N_D - N_A)^2 + 4n_i^2}\right] \tag{4.23}$$

If $\left|N_D - N_A\right| >> n_i^2$ and $N_D >> N_A$ Equation (4.23) reduces to

$$n_{n0} = N_D, \tag{4.24}$$

and

$$p_{no} = \frac{n_i^2}{n_{n0}} \approx \frac{n_i^2}{N_D} . \tag{4.25}$$

The concentration of the holes and electrons on the p side with the combination of same equations is given by the

$$p_{p0} = \frac{1}{2}\left[\left(N_A - N_D\right) + \sqrt{(N_A - N_D) + 4n_i^2}\right], \tag{4.26}$$

if $\left|N_A - N_D\right| >> n_i^2$ and $N_A >> N_D$ Equation (4.25) reduces to

$$p_{p0} = N_A, \tag{4.27}$$

and

$$n_{p0} = \frac{n_i^2}{p_{p0}} \approx \frac{n_i^2}{N_A}. \tag{4.28}$$

With the help of Equation (4.28) far from the junction on the p side

$$n(-\infty) = \frac{n_i^2}{N_A}, \tag{4.29}$$

and similarly far from the junction on the n side

$$n(+\infty) = N_D. \tag{4.30}$$

We can write built in potential by using these boundary conditions and Equation (4.21) as

$$V_{bi} = \frac{kT}{q} \ln\left[\frac{n(+\infty)}{n(-\infty)}\right], \tag{4.31}$$

Or by substituting Equations (4.29) and (4.30) into Equation (4.31)

$$V_{bi} = \frac{kT}{q} \ln\left[\frac{N_D N_A}{n_i^2}\right]. \tag{4.32}$$

4.1.5. Depletion Approximation

The quantitative solutions for the charge density, E, and $V(x)$ across the p-n junction under thermal equilibrium conditions are centered around the solutions of Poisson's equation as given by Equations (4.6) and (4.7). In general E, V, n, N_D and N_A are functions of x, except for uniform doping where N_D and N_A are constants. Poisson's equation in its exact form is not easily solved for most devices because p and n are in turn functions of V and E, the unknowns. To solve the equation in closed form it is necessary to make several simplifications. A particularly useful set of simplifications that allow the solution of Poisson's equation to be obtained explicitly are collectively called the depletion approximation. The depletion

approximation is stated below with three constraints;

$N_A >> n_p$ or p_p, hence $\rho = -qN_A$ for $-x_p \le x \le 0$.

$N_D >> n_n$ or p_n, hence $\rho = qN_D$ for $0 \le x \le x_n$.

The charge density is zero in bulk regions; that is, for $x > x_n$ and $x < -x_p$.

The depletion region is bounded by $-x_p$ and x_n, while the regions outside the depletion region are called the n and p bulk regions respectively.

4.1.6. The Ideal Diode Equation

This section develops a ‘’game plan’’ for the quantitative solution of the basic semiconductor equations as applied to the abrupt p-n junction. The eventual goal is to derive a first order relationship for the I versus V_A dependence of the p-n junction, known as the ideal diode equation. Several assumptions about the device are invoked to make $I - V_A$ solution tractable.

- There are no external sources of generation, for example no light.
- The depletion approximation and the step junction are applicable.
- The steady state dc solution is desired; that is, all the d/dt terms are zero.
- No generation or recombination takes place in the depletion region.
- Low-level injection is maintained in the bulk regions.
- The electric field for the minority carriers is zero in the bulk regions.
- The bulk regions are uniformly doped; that is, N_A and N_D are constants.

The general form of the continuity equations for electrons and holes respectively are given by

$$\frac{\partial n}{\partial t} = G_n - U_n + \frac{1}{q}\nabla \cdot J_n, \tag{4.33}$$

and

$$\frac{\partial p}{\partial t} = G_p - U_p - \frac{1}{q}\nabla \cdot J_p, \tag{4.34}$$

G_n and G_p are the electron and hole generation respectively. U_n and U_p are the recombination rates. Under low injection conditions (when the injected carrier density is much less than the equilibrium majority carrier density) U_n can be approximated by expressions $(n_p - n_{p0})/\tau_n$ where n_p is the minority carrier density, n_{p0} the thermal equilibrium minority carrier density, and τ_n the electron lifetime. There is a similar expression for the hole recombination rate with lifetime τ_p.

With the assumptions given above the equations of continuity for the bulk n and p region reduce to the following minority carrier equations,

$$-\frac{(n_p - n_{p0})}{\tau_n} + \frac{1}{q}\nabla \cdot J_n = 0, \tag{4.35}$$

and

$$-\frac{(p_n - p_{n0})}{\tau_p} - \frac{1}{q}\nabla \cdot J_p = 0. \tag{4.36}$$

Using the Equation (4.14) and the fact that the electric field for the minority carriers is zero in the bulk regions the Equation (4.36) reduces to

$$\frac{\partial^2 p_n}{\partial x^2} - \frac{p_n - p_{n0}}{D_p \tau_p} = 0. \tag{4.37}$$

In order to solve Equation (4.37) we have to set boundary conditions at x_n and x_p. When V_A is applied across the terminals of the diode, the junction potential V_j is equated to $V_{bi} - V_A$ under the assumption that electric field is essentially zero in the bulk regions. The assumption of ''low-level injection'' suggests that in the depletion region the additional currents due to the applied voltage are also small. In the depletion region $E = 0$ and the electron current is the difference between the large

current density components, as given with Equation (4.14). Also it is assumed that E and n has not changed much under low-level injection and Equation (4.14) turns into Equation (4.16).

By using Equation (4.19) and the definition of potential, the junction voltage can be written as

$$V_j = V_{bi} - V_A = -\int_{-x_p}^{x_n} E dx . \tag{4.38}$$

Substituting Equation (4.18) into Equation (4.38) yields

$$V_{bi} - V_A = \frac{kT}{q} \ln \frac{n(x_n)}{n(-x_p)} . \tag{4.39}$$

Inverting Equation (4.39) by cross multiplying and raising both sides to the exponential, we get the electron concentration;

$$n(x_n) = n(-x_p) e^{[+qv_{bi}/kT]} e^{[-qV_A/kT]} . \tag{4.40}$$

By using Equation (4.32) with Equations (4.24) and (4.27) and deriving $e^{-qV_{bi}/kT}$ as $\frac{n_i^2}{n_{n0} p_{p0}}$ electron concentration given by Equation (4.40) can be written as

$$n(-x_p) = n(x_n) \frac{n_i^2}{n_{n0} p_{p0}} e^{qV_A/kT} . \tag{4.41}$$

For low level injection the change in majority carrier in the bulk region can be neglected. Therefore $n(x_n) = n_{n0}$. Using the condition given for low level injection and the fact given by Equation (4.22) Equation (4.41) reduces to

$$n(-x_p) = n_{p0} e^{qV_A/kT} , \tag{4.42}$$

and the excess electron concentration at $-x_p$ is

$$\Delta n(-x_p) = n(-x_p) - n_{p0} = n_{p0}(e^{qV_A/kT} - 1)\,. \tag{4.43}$$

Complementary arguments can be used for the hole concentration at the edges of the depletion regions and result in

$$\Delta p(x_n) = p_{n0}(e^{qV_A/kT} - 1) \tag{4.44}$$

4.1.7. Long Base Diode

The final boundary conditions on the excess carrier concentration in the p and n bulk regions are obtained by assuming that the bulk regions are very long, infinite, in length. Since the excess minority carriers have a finite lifetime (τ_p and τ_n), they cannot survive forever without recombining; consequently,

$$\Delta n_p(-\infty) = 0\,, \tag{4.45}$$

and

$$\Delta p_n(\infty) = 0\,. \tag{4.46}$$

After the definition of boundary conditions Equation (4.37) can be solved as by change of variable as setting the variable given below

$$\Delta p_n = p_n - p_{n0}\,, \tag{4.47}$$

with the help of Equation (4.47) Equation (4.38) reduces in to

$$\frac{d^2\Delta p_n(x)}{dx^2} - \frac{\Delta p_n(x)}{\tau_p D_p}\,. \tag{4.48}$$

By setting $\sqrt{D_p\tau_p}$ as diffusion length L_p Equation (4.48) is a very common differential equation can be solved directly. The solution is of the form

$$\Delta p_n(x) = A_1 e^{x/L_p} + A_2 e^{-x/L_p} \tag{4.49}$$

Where two boundary conditions are needed to evaluate constants A_1 and A_2. From Equation (4.46), the boundary condition at infinity requires

$$\Delta p_n(\infty) = A_1 e^{\infty} + A_2 e^{-\infty} = 0\,. \tag{4.50}$$

Equation (4.50) satisfied only if $A_1 = 0$. Boundary condition given by Equation (4.44) requires;

$$A_2 = p_{n0}(e^{qV_A/kT} - 1)e^{x_n/L_p}, \tag{4.51}$$

then Equation (4.50) becomes

$$\Delta p_n = p_{n0}(e^{qV_A/kT} - 1)e^{-(x-x_n)/L_p}\,. \tag{4.52}$$

To set the diffusion currents Equation (4.12) and Equation (4.13) can be called back with the boundaries at $x = x_n$ and $x = -x_p$. Than the diffusion current densities can be written in the forms given below

$$J_n = +qD_n \frac{\partial n_p}{\partial x}\Big|_{-x_p}, \tag{4.53}$$

and

$$J_p = -qD_p \frac{\partial p_n}{\partial x}\Big|_{x_n}. \tag{4.54}$$

By using Equation (4.52) with the Equation (4.54) the diffusion current density of the minority carriers on p side becomes

$$J_p = \frac{qD_p p_{n0}}{L_p}(e^{qV_A/kT} - 1)\,, \tag{4.55}$$

similar derivations for minority carriers on n side can be done and diffusion current density is obtained as;

$$J_n = \frac{qD_n n_{p0}}{L_n}(e^{qV_A/kT} - 1)\,. \tag{4.56}$$

As given in Equation (4.15) the total diffusion current density becomes;

$$J = \left(\frac{qD_p p_{n0}}{L_p} + \frac{qD_n n_{p0}}{L_n}\right)(e^{qV_A/kT} - 1)\,, \tag{4.57}$$

under any reasonable amount of forward bias, the exponential term is much greater than -1 and Equation (4.57) reduces to:

$$J = \left(\frac{qD_p p_{n0}}{L_p} + \frac{qD_n n_{p0}}{L_n}\right)(e^{qV_A/kT})\,. \tag{4.58}$$

4.1.8. Forward Bias Deviations from Ideal and Recombination in the Depletion Region

Non ideal region is considered at very small values of forward current. In this region of operation the injected carrier densities are relatively small and holes leaving the p region travel through the depletion region on their way to be injected as minority carriers into the n region. Simultaneously, electrons are traveling from the n region through depletion region to be injected into p region. The ideal diode equation assumed that no recombination-generation occurs in the depletion region. With the carrier numbers being greater than their thermal equilibrium values, recombination can occur in the depletion region which is width is symbolized by W. Each recombination event removes an excess electron and hole. For ideal diode, the currents injected were determined by the excess carriers at the edges of the depletion region. The excess carriers at the depletion region edges were determined by the applied voltage V_A.

The electrons recombine with the holes from the p region with the holes, thereby forming a recombination current density component of the total current density. The recombination current density component is added to the ideal diode diffusion current densities. The recombination rate denoted by U is given by;

$$U \approx \frac{1}{2}\sigma v_{th} N_t n_i \exp\left(\frac{qV_A}{2kT}\right), \tag{4.59}$$

where σ, v_{th} , N_t denote capture cross section, carrier thermal velocity and trap density respectively.

Recombination current density in the depletion region is defined as;

$$J_{rec} = \int_0^W qUdx\,. \tag{4.60}$$

By substituting Equation (4.59) into Equation (4.60) recombination current density can be defined as;

$$J_{rec} = \frac{qW}{2}\sigma v_{th} N_t n_i \exp\left(\frac{qV_A}{2kT}\right) \tag{4.61}$$

Than the total forward current density is written by summing diffusion current density given by Equation (4.58) and the recombination current density given by Equation (4.61)

$$J_F = \left(\frac{qD_p p_{n0}}{L_p} + \frac{qD_n n_{p0}}{L_n}\right)(e^{qV_A/kT}) + \frac{qW}{2}\sigma v_{th} N_t n_i e^{qV_A/2kT}\,. \tag{4.62}$$

Since diffusion length given by $\sqrt{D_p \tau_p}$ Equation (4.62) can be expressed as;

$$J_F = q\left(\sqrt{\frac{D_p}{\tau_p}} p_{n0} + \sqrt{\frac{D_n}{\tau_n}} n_{n0}\right)(e^{qV_A/kT}) + \frac{qW}{2}\sigma v_{th} N_t n_i e^{qV_A/2kT}\,. \tag{4.63}$$

Equation (4.63) reduces into the form with the fact that majority of LEDs dominant radiative recombination occurs only one side of the junction especially on the p side (Tyagi, 1934).

$$J_F = q\left(\sqrt{\frac{D_p}{\tau_p}}\frac{n_i^2}{N_D}\right)(e^{qV_A/kT}) + \frac{qW}{2}\sigma v_{th}N_t n_i e^{qV_A/2kT}\ . \tag{4.64}$$

The experimental results can be represented by the following empirical form

$$J_F \approx \exp\left(\frac{qV}{nkT}\right). \tag{4.65}$$

Where the factor $n = 2$ when the recombination current dominates, and $n = 1$ when the diffusion current dominates. When both currents are comparable, n has a value between 1 and 2.

4.1.9. Bulk Region Effects

In the derivation of the ideal diode equation, it was assumed that the electric field in the bulk n and p regions was approximately zero and no voltage drop existed across the ohmic contacts. For most modern devices these are good assumptions at the lower current levels. However, at large current levels the bulk resistance can produce a significant voltage drop an the applied voltage V_A is larger than the voltage across the depletion region. Also, metal contact behaves as a small resistor adding to the voltage drop across n and p regions. Usually these two effects are combined into resistor R_s, the series resistance.

One method to calculate series resistance is adding the series resistance voltage drop effect to current mechanism as;

$$I = I_0\left(e^{q(V_A - IR_s)/(n\ kT)}\right). \tag{4.66}$$

The series resistance can be evaluated at high voltage where $V_A > E_g / q$.Solving Equation (4.66) for V_A and then differentiating V_A with respect to I yields;

$$\frac{dV_A}{dI} = R_s + \frac{n\ kT}{q}\frac{1}{I}, \tag{4.67}$$

where the first summand on the right hand side of the equation represents the differential p-n junction resistance (Schubert, 2003).

4.1.10. Junction Capacitance

Unlike parallel plate capacitance, which is constant, the junction capacitance changes with the applied dc voltage. The capacitance decrease as V_A becomes more negative. To explain this phenomenon, the depletion region at some fixed value or reverse voltage is considered. For a linearly graded junction the depletion region width is determined by defining the electric field and built in potential in the depletion region. In this type of junction it is considered that p impurities thermally diffused into n substrates. If a straight line has a slope of ''-a'', then impurity distribution can be described by;

$$N_A(x) - N_D = -ax, \tag{4.68}$$

where "a" has the units of number/cm4 and is called the grading constant.
The depletion approximation, as applied to the graded junction, the charge density can be given by

$$\begin{aligned} &\rho = qax \text{ for } -x_p \le x \le x_n, \\ &\rho = 0 \qquad \text{elsewhere.} \end{aligned} \tag{4.69}$$

The symmetry of the linearly graded charge density simplifies the solution because by inspection we must have $x_p = x_n = W/2$.

To solve Equation (4.6) with the charge density given by Equation (4.69) reduces to

$$\begin{aligned} &E(x) = \frac{qa}{2K_s\varepsilon_0}\left[x^2 - (W/2)^2\right] \text{ for } -W/2 \le x \le W/2 \\ &E = 0 \qquad\qquad\qquad\qquad \text{elsewhere,} \end{aligned} \tag{4.70}$$

with the fact that $E(-x_p)=E(x_n)=0$.
With the help of Equation (4.7) since the boundary conditions are given as $V(-x_p) = 0$ and $V(x_n) = V_{bi}$, potential across the depletion region can be derived as;

$$V(x) = \frac{qa}{6K_s\varepsilon_0}\left[2\left(\frac{W}{2}\right)^3 + 3\left(\frac{W}{2}\right)^2 x - x^3\right] \quad -\frac{W}{2} \le x \le \frac{W}{2}, \tag{4.71}$$

and depletion region is given by

$$W = \left[\frac{12K_s\varepsilon_0}{qa}(V_{bi} - V_A)\right]^{1/3}, \tag{4.72}$$

here built in potential is defined by using Equation (4.32) and the donor and acceptor concentration definition given by $N_A = N_D = \frac{aW}{2}$,

$$V_{bi} = \frac{2kT}{q}\ln\left[\frac{aW}{2n_i}\right]. \tag{4.73}$$

As there are similarities between the parallel plate capacitor and the junction capacitance, the junction capacitance is given by

$$C_j = \frac{K_s\varepsilon_0 A}{W}. \tag{4.74}$$

Using Equation (4.74) and the depletion width given for linearly graded junction in Equation (4.72) a simple equation can be derived for junction capacitance as

$$C_j = \frac{K_s\varepsilon_0 A}{\left[\frac{12K_s\varepsilon_0}{qa}(V_{bi} - V_A)\right]^{1/3}}. \tag{4.75}$$

If $|V_A| >> V_{bi}$

$$C_j \propto \frac{1}{|V_A|^{1/3}}. \tag{4.76}$$

4.2. The Effects of Defect

The previous parts of this chapter were concerned with the electrical properties of a

p-n junction. The current mechanism was explained in a detailed way. This section will demonstrate the microscopic view of the damage produced by gamma irradiation and also show the defects affect the macroscopic electrical parameters such as carrier concentration, mobility, conductivity and lifetime. As indicated in section (4.2.8) whenever the thermal equilibrium conditions of a physical system are distributed there are processes by means of which the system tends to revert to equilibrium. The mechanism that restores the equilibrium, recombination shall be treated in some detail here since it will be important in considering radiation effects on carrier lifetime.

The proposed kinetic models for carrier recombination in a semiconductor include recombination through a trap and band-to-band recombination (Blakemore, 1962). In trap recombination, the recombination process is aided by deep level impurities. As is suggested by its name, band-to-band recombination is the direct recombination of an electron and a hole.

There are several subclasses in each of the recombination models. The subclasses refer to means of removing the excess energy when recombination occurs. When an electron is captured on a deep trap, for example an energy that is the difference between initial and final electron energies must be removed from the electron. The energy may be removed in the form of photon (radiative recombination), or in a series of phonons as the electron cascades down in energy through excited states of the center (Lax, 1959); or the electron may give its energy to another electron (Landsberg and Beattie, 1959). In addition combination of these processes always possible.

Most of these mechanisms for removal of energy can also apply to band-to-band recombination. In particular, radiative and Auger processes may occur in just the same manner as in electron capture on a trap. The loss of energy through multiple phonons seems quite unlikely in band-to-band recombination, but an electron hole complex may be formed by the emission of a single phonon. The excitation can then recombine radiatively or by the Auger process. It is also possible that a recombination process is clearly characteristic neither of band-to-band recombination through traps.

Recombination through traps dominates the carrier lifetime in germanium, silicon and many compound semiconductors. For a given disturbance in carrier density, there will be a rate of recombination which depends on the magnitude of the disturbance and the mechanism of recombination. The lifetime is defined as;

$$\tau_n = \frac{\Delta n}{dn/dt}, \tag{4.77}$$

where τ_n is electron lifetime, Δn excess number of electrons and dn/dt is the rate of disappearance of electrons by recombination centers.

4.2.1. Recombination through a Single Level Trap

The problem of calculating carrier lifetime is reduced by Equation (4.77) to the calculation of the rate of recombination, dn/dt, as a function of excess electron density. At steady state, the rate of recombination of electrons as well as the rate of recombination of holes must be equal. Single level acceptor type trap is assumed. The four processes that can occur are electron recombination on a neutral acceptor, electron generation from a negative acceptor, hole recombination on a negative acceptor, and hole generation from a neutral acceptor.

The average free time for electrons before capture is

$$\tau_{1n} = \frac{1}{v_t \sigma_n N_T^0}. \tag{4.78}$$

And the average free time for holes is,

$$\tau_{1p} = \frac{1}{v_t \sigma_p N_T^-}, \tag{4.79}$$

where N_T^0 and N_T^- are the number of neutral and number of negatively charged traps respectively. The escape times for captured electrons and holes can be given by

$$\tau_{2n} = \frac{1}{v_t \sigma_n n_1}$$
$$\tau_{2p} = \frac{1}{v_t \sigma_p p_1}, \tag{4.80}$$

where n_1 and p_1 are electron and hole densities that would be obtained if the Fermi level were at trap level.

With the departure from equilibrium obtained by generation of electron-hole pairs, a steady state nonequilibrium density of electrons and holes is obtained. In addition, the state of charge of the trap is altered. The equations that describe the steady state departure from equilibrium are;

net rate of recombination of electrons:

$$\frac{dn}{dt} = -\frac{n}{\tau_{1n}} + \frac{N_T^-}{\tau_{2n}}. \tag{4.81}$$

By using the average free time for electrons before capture and escape time for captured electrons Equation (4.81) reduces into

$$\frac{dn}{dt} = -v_t \sigma_n (n N_T^0 - n_1 N_T^-). \tag{4.82}$$

The net rate of recombination of holes can be written in a same manner as

$$\frac{dp}{dt} = -\frac{p}{\tau_{1p}} + \frac{N_T^0}{\tau_{2p}}, \tag{4.83}$$

and using the definitions given by Equations (4.79) and (4.80) Equation (4.83) becomes

$$\frac{dp}{dt} = -v_t \sigma_p (p N_T^- - p_1 N_T^0). \tag{4.84}$$

From the conservation of traps given by

$$N_T^- + N_T^0 = N_T \,. \tag{4.85}$$

The rate of change of charge on the traps at steady state is given as;

$$0 = v_t \sigma_n (n N_T^0 - n_1 N_T^-) - v_t \sigma_p (p N_T^- - p_1 N_T^0) \,. \tag{4.86}$$

Equations (4.85) and (4.86) can be solved as linear equations in N_T^0 and N_T^- to obtain the steady state charge on traps. The numbers of neutral and negative traps are found to be,

$$\begin{aligned} N_T^0 &= N_T \frac{\sigma_p p + \sigma_n n_1}{\sigma_n (n + n_1) + \sigma_p (p + p_1)} \\ N_T^- &= N_T \frac{\sigma_n n + \sigma_p p_1}{\sigma_n (n + n_1) + \sigma_p (p + p_1)} \,. \end{aligned} \tag{4.87}$$

For the sake of simplicity the radiation induced-defects produce a single energy level in the forbidden energy gap of the semiconductor is assumed and also it is assumed that the defect is an acceptor level and that is located above midgap $\varepsilon_T > \varepsilon_i$ in n type material. Here ε_T is defect energy level and ε_i is the midgap energy.

For the assumptions listed above $n >> p$ and $n_1 >> p_1$ Equation (4.87) reduces to (Chaffin,1973),

$$\frac{N_T^-}{N_T} = \frac{n}{n + n_1} \,. \tag{4.88}$$

For a deep trap $\varepsilon_T << \varepsilon_C$ and hence $n_1 << n$ Equation (4.88) reduces to (Series expansion)

$$N_T^- \cong N_T \left(1 - \frac{n_1}{n} \right). \tag{4.89}$$

Knowing that the n_1 was given by Equation (4.4) when the trap level at Fermi level

and for low level injection that corresponds to $\Delta n << n_0$ and Δn can be ignored while writing electron concentration in the case of non-thermal equilibrium. Substituting the n_1 and n with the assumptions given above Equation (4.89) can be written as;

$$N_T^- = N_T\left[1-\exp\left(\frac{\varepsilon_T-\varepsilon_f}{kT}\right)\right], \tag{4.90}$$

here N_T^- trapped electrons. Initially the free electron concentration (assumed n type material) is given by $n \cong N_D$.In the post irradiated case some of the electrons are tied up in traps, and, therefore the free electron concentration for this case may be approximated by

$$n = N_D - N_T\left[1-\exp\left(\frac{\varepsilon_T-\varepsilon_f}{kT}\right)\right]. \tag{4.91}$$

If the density of introduced traps is proportional to the radiation fluence, then (Chaffin, 1973)

$$N_T = B.\Phi, \tag{4.92}$$

where, B is a constant and Φ is the radiation fluence of any type. Substituting Equation (4.90) into Equation (4.91), it can be seen that the free majority carrier density is reduced by the radiation fluence. This effect is called carrier removal and is usually given in terms of carrier removal rate.

Using Equation (4.91) and Equation (4.92) carrier removal rate for the case is given by

$$\frac{\Delta n}{\Delta\Phi} = -B\left[1-\exp\left(\frac{\varepsilon_T-\varepsilon_f}{kT}\right)\right]. \tag{4.93}$$

In order to consider the effect of radiation-induced single acceptor level on minority-carrier lifetime, the low level minority carrier lifetime is given by (Chaffin, 1973;

Sze, 1969)

$$\tau_p \cong \frac{1}{N_T v_t \sigma_p}, \tag{4.94}$$

v_t is the velocity of electrons and holes traveling through the lattice, and σ_p is capture cross section of hole to be captured by the trap. The degradation in minority carrier lifetime is usually expressed as (Share et al, 1975; Barnes, 1979; Onoda et al, 2001; Chaffin, 1973)

$$\Delta\left(\frac{1}{\tau}\right) = \frac{1}{\tau_f} - \frac{1}{\tau_0} = K_\tau \Phi, \tag{4.95}$$

where τ_f is the lifetime after irradiation and τ_0 is the lifetime before irradiation. K_τ is the lifetime damage constant. The lifetime degradation rate is simply (Chaffin, 1973)

$$\frac{\Delta(1/\tau)}{\Delta\Phi} = K_\tau \tag{4.96}$$

An attempt to fit the change of current mechanism given by Equation (4.64) with respect to damage effects the degradation of p-n junction diode performance is known to be caused by the decrease of minority carrier lifetimes which is given by Equation (4.95) and repeated here for holes and electrons respectively,

$$\frac{1}{\tau_p} = \frac{1}{\tau_{p0}} + K_p \Phi, \frac{1}{\tau_n} = \frac{1}{\tau_{n0}} + K_n \Phi. \tag{4.97}$$

To understand the radiation damage to current mechanism lifetime degradation has a great importance. Combining the Equations (4.64) and (4.95) gives the radiation effect on diffusion current mechanism as;

$$I_D = I_{D0}\sqrt{1 + K_p \tau_{p0} \Phi}\, \exp\left(\frac{qV_A}{kT}\right), \tag{4.98}$$

here, I is the diffusion current which can be get from diffusion current density given

by Equation (4.58).

Radiation damage effect on series resistance can be analyzed by using the definition of conductivity;

$$\sigma_p = q(\mu_p p), \tag{4.99}$$

Since the series resistance is a function of conductivity and the conductivity is a function of mobility it is well to write the mobility degradation. The damage of radiation on mobility is given as;

$$\Delta\left(\frac{1}{\mu}\right) = \frac{1}{\mu_f} - \frac{1}{\mu_0}, \tag{4.100}$$

where μ_f and μ_0 are the mobilities after and before irradiation. The mobility degradation rate is given by (Chaffin, 1973)

$$\frac{\Delta(1/\mu)}{\Delta\Phi} = \frac{B\left(1 - \exp\left[\left(\varepsilon_T - \varepsilon_F\right)/kT\right]\right)}{C}, \tag{4.101}$$

here B and C are constants. Since radiation-produced defects introduce a multitude of energy levels in the forbidden gap (Corbett, 1966; Watkins, 1968) the analysis of the effects of a single energy level can be enlarged in order to understand the radiation defects in the real world. Mathematical analysis of this problem is very difficult by lack of data concerning the exact values of the energy levels and the correct values of the capture cross sections.

CHAPTER 5

EXPERIMENTAL METHODS

In this chapter in order to analyze gamma damage effects in LEDs two types of LEDs were selected for this study as shown in Table 1. They are simple and low-cost diffused LEDs. The devices examined in this work were GaP (green) and GaAsP (red) light emitting diodes (manufactured by SUNLED Company) with the emission wavelength given by Table 1.

GaP has an indirect band gap of 2.26 eV at 300K. It can be made p- and n- type by using appropriate dopants. A green colored LED with $\lambda = 565nm$ can be achieved by using nitrogen impurity with both the p and n sides of the junction are doped.
A red LED can be obtained by doping with zinc and oxygen, as the nearest neighbor pairs gives rise to red emission with $\lambda = 690nm$ .The GaAs1-yPy compound behaves as a direct band gap semiconductor for $y \leq 0{,}45$ and has a indirect gap for larger values of y. In order to study the LED devices were irradiated with gamma rays emitted from 10kCi 60Co source at Ankara Nuclear Research Center. The dose rate of the source is 1.85kGy/h. The following light emitting diode properties were measured; forward I-V, C-V characteristics and peak spectral intensity, L. The parameters were measured before irradiation and after each ^{60}Co irradiation for the doses given as 493Grey, 986Grey, 9866Grey, 33.3×10 3 Grey, 75.9×10 3 Grey and 400×103 Grey.

All irradiation was performed with open circuit devices to reduce bias annealing effects, which can occur for devices biased during irradiation. Since the LEDs were not same for each measurement, it is impossible to show the characteristics on the same plot. From the observed fact the slight changes up to doses 33.3×10 3 Grey, the following graphs were plotted for the last total dose where the maximum deviation occurs in order to analyze the changes.

Table 1. The basic properties of LEDs investigated in this study

Part Number	Emitting Color	Emitting Material	Lens Color	Wavelength (nm)
XLUG53D	Green	GaP	Green Diffused	565
XLUR53D	Red	GaAsP/GaAs	Red Diffused	627

5.1. Error Analysis

No measurement can yield one absolutely true value. Rather, the best we can hope for is a best estimate. In addition, we can collect enough information to tell us how sure we can be of our best estimate.

We expand our analysis of error computation and error propagation to include the important case of statistically independent errors which are normally distributed (distributed according to Gaussian distribution).

Let X be the physical quantity we are interested in. Let $\overline{X}$ stand for the numerical value of quantity X and let δX stands for the precision. We will write

$$X = \overline{X} \mp \delta X \ . \tag{5.1}$$

We shall assume that errors are entirely random in nature, that they are not systematic or the result of sloppy measurements. We will show, assuming random nature of the results of measurements that the best possible choice for $\overline{X}$ is the arithmetic mean of the set of measured values and that δX is the standard deviation of the mean.

Suppose a quantity X is measured many times, say N times. Each measurement result is denoted by X_i where index $i = 1,2,...,N$. If the results of measurements occur randomly, then the probability distribution that describes the measurements is known as the ``normal distribution'' or Gaussian distribution. The Gaussian

distribution is constructed such that the most probable value, the peak is at the location of the average.

Let X_t stand for the true value of the variable being measured. Then, each individual measurement differs from the true value by an amount $\varepsilon_i = X_i - X_t$ called the deviation. In reality we do not know the true value of the variable. However, we can ask the question what is the best possible approximation X_b of the true value?

Assuming that we have found the best possible approximation X_b then we can measure the deviations relative to it. We write the deviation of the measurement from the best approximation as $\varepsilon_i = X_i - X_b$. To find the best possible approximate value we consider the cumulative quadratic error also known as cumulative variance. It is defined by

$$M = \sum_{i=1}^{N} (X_i - X_b)^2 \,. \tag{5.2}$$

The cumulative variance is minimal if the arithmetic average is taken as the best probable value, the approximation of the true value. The cumulative variance is a function of the variable X_b. We calculate the minimum value of the cumulative variance to determine X_b. The condition that the cumulative variance is minimal is that its first derivative with respect to X_b vanishes:

$$\frac{\partial M}{\partial X_b} = 0 = -2\sum_{i=1}^{N} (X_i - X_b) \,. \tag{5.3}$$

This equation is easy to solve. First, we transform the equation into

$$\sum_{i=1}^{N} X_i = NX_b \,. \tag{5.4}$$

The solution reads,

$$X_b = \bar{X} = \frac{1}{N}\sum_{i=1}^{N} X_i \,. \tag{5.5}$$

Also, the second derivative of the cumulative variance is positive. This implies that the extreme point is the minimum.

It is convenient to introduce average variance, or just variance, as a quadratic measure of the deviation. It is defined with respect to average,

$$V = \frac{1}{N}M = \frac{1}{N}\sum_{i=1}^{N}(X_i - X_b)^2 = \frac{1}{N}\sum_{i=1}^{N}(X_i - \bar{X})^2 \,. \tag{5.6}$$

The Standard deviation, also called, root mean square, (rms), is defined in terms of the variance as

$$\sigma = \sqrt{\frac{N}{N-1}V} = \sqrt{\frac{\sum_{i=1}^{N}(X_i - X_b)^2}{N-1}} = \sqrt{\frac{\sum_{i=1}^{N}(X_i - \bar{X})^2}{N-1}} \,. \tag{5.7}$$

The error of the average is given by

$$\delta X = \sqrt{\frac{1}{N^2}\sum \sigma^2} = \frac{\sigma}{\sqrt{N}} \,. \tag{5.8}$$

This can also be written as

$$\delta X = \frac{\sigma}{\sqrt{N}} = \sqrt{\frac{\sum_{i=1}^{N}(X_i - \bar{X})^2}{N(N-1)}} \,. \tag{5.9}$$

The last result is an important formula for we will write that the measured value of some quantity X is best approximated by the arithmetic average of the results of the measurements. The error we will quote is the error of the average.

5.2. I-V Measurement

The current voltage measurements are important, because it enables us to determine change in the characteristics. In order to record I-V characteristics, following experimental set up was used.

Voltage is supplied to the LED by the Hewlett Packard 4140B pA meter/DC voltage source. 4140B pA meter/DC source can apply voltage while measuring the current response of the LED. It can deliver a potential difference across its terminals in the range -100V to 100V with maximum resolution of 10mV. It has measurement capability for current between 10fA to 10mA. The I-V measurements are done at the room temperature and automatically recorded by the help of Labview software. The I -V characteristics are given by Figure 5, Figure 6 for the LEDs with the part numbers XLUG53D, XLUR53D.

For the reliability of the measurements and in order to reduce experimental error, every measurement was repeated three times. The best possible approximation of the voltage values and the error of the averages are calculated by using Equation (5.5) and Equation (5.9). The maximum error for the current is 15×10-5 A. Using the error in voltage difference ±10mV and the error in currents, best and worst lines are plotted. With the use of best and worst lines error in slope is found to be (0.9 and error for ideality factor becomes 0.10).

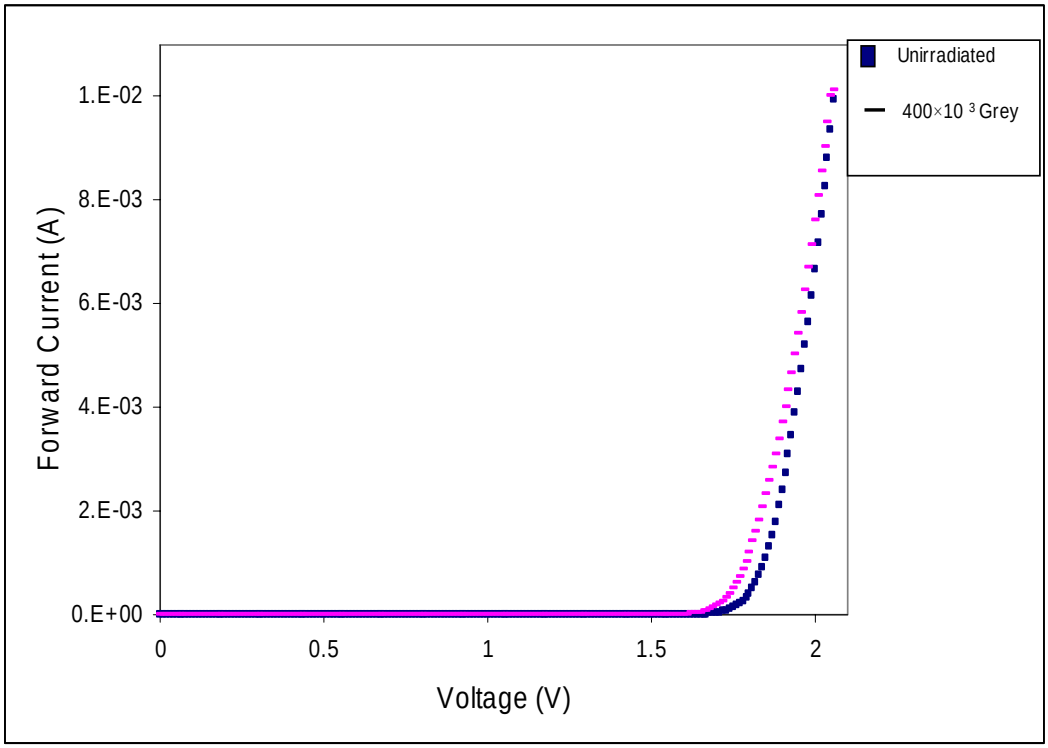

Figure 5. Forward current versus voltage of LED with a part number XLUG53D.

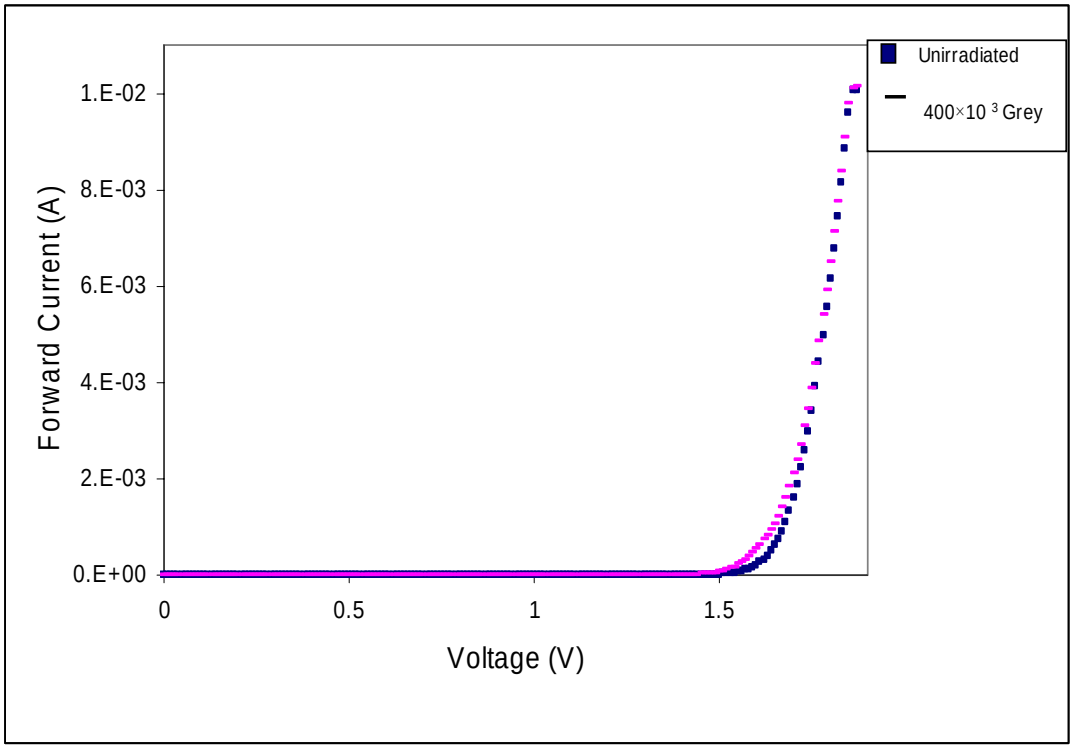

Figure 6. Forward current versus voltage of LED with a part number XLUR53D.

5.3. C-V Measurement

In order to have information about dopant concentration, determination of C-V characteristics is important.

Measurements of capacitances are carried using a Hewlett Packard 4192A LF impedance analyzer. A impedance analyzer over a frequency range of 5Hz-13MHz interfaced a computer using Labview software for data collection.

The measurements are made in the room temperature. For applied voltages ranging from 2V to -10V the capacitance values were recorded at 1MHz. The C-V characteristics are given by Figure 7, Figure 8 for the LEDs with the part numbers XLUG53D and XLUR53D. The maximum error for the capacitance is 1.76×10-13 F.

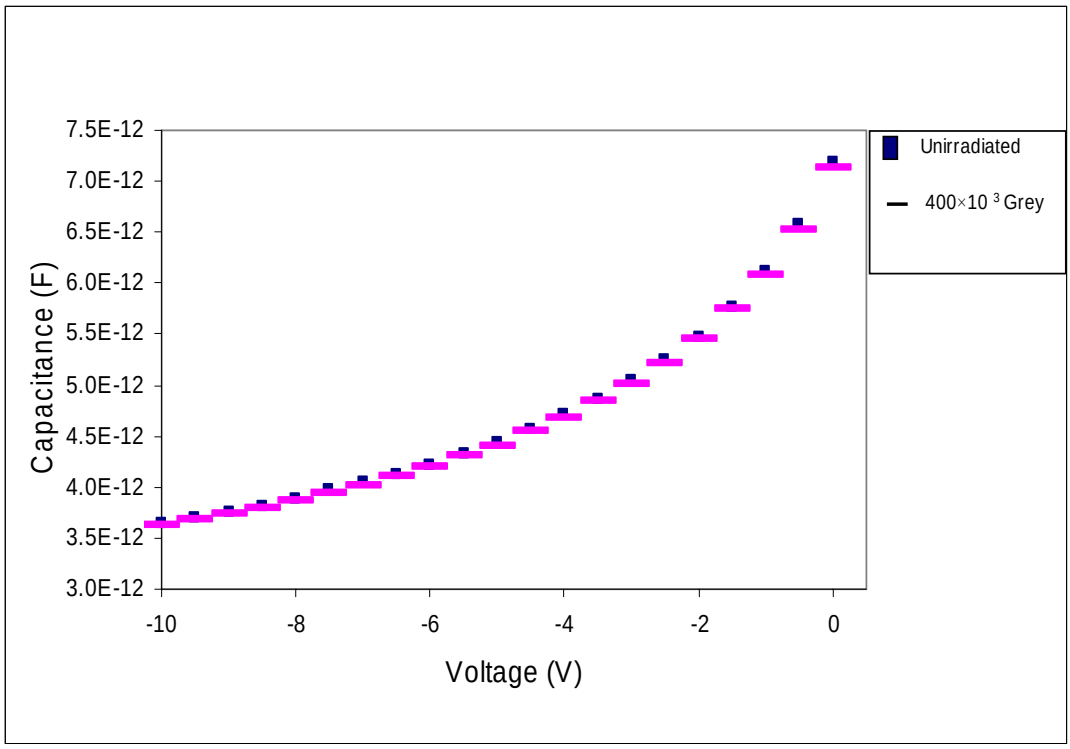

Figure 7. Capacitance versus voltage of LED with a part number XLUG53D (green) before and after irradiation

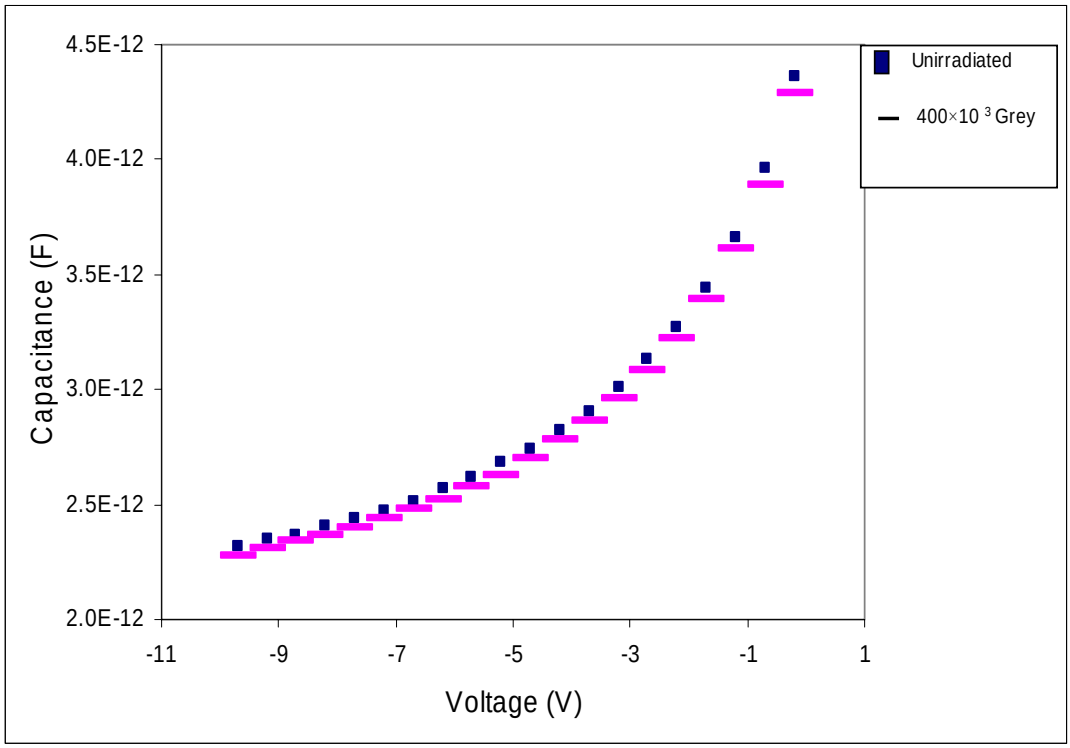

Figure 8. Capacitance versus voltage of LED with a part number XLUR53D (red) before and after irradiation.

5.4. Spectral Response

Here emission spectra were measured with HR2000 spectrometer The HR2000 High-resolution Miniature Fiber Optic Spectrometer is a small-footprint, modular spectrometer with optical resolution to 1 nm.

The HR2000 is especially suited for applications such as wavelength characterization of lasers and LEDs, monitoring of gases and monochromatic light sources, and determination of elemental atomic emission lines.

A schematic construction for wavelength characterization of LEDs is given by Figure 9. HR200 is operating in the 200 to 1100-nm range

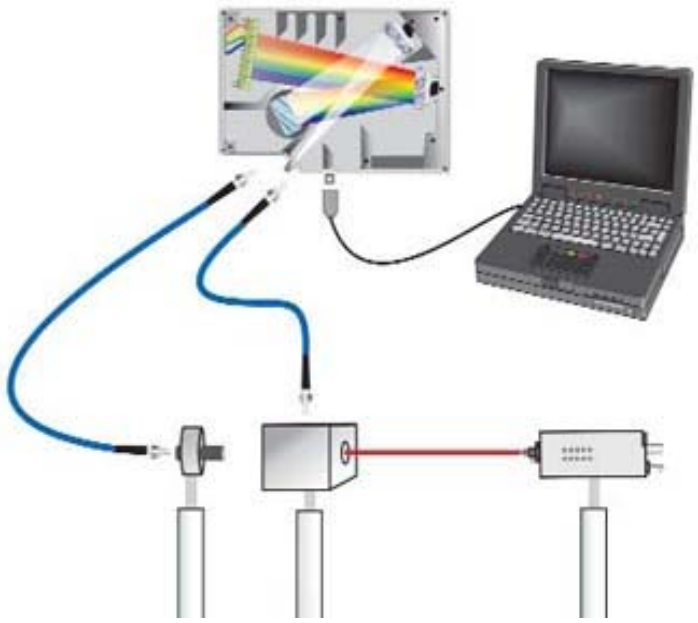

Figure 9. Schematic construction for wavelength characterization.

During the measurement, LEDs were biased by using a voltage source with 5V output. The spectral responses respectively for XLUG53D and XLUR53D are given in Figures 10 and 11.

In this part error calculation was made with a procedure same as given in sections (5.3) and (5.4). The maximum error for the intensity is ±40 arbitrary units and the corresponding error for peak wavelength is ±7nm.

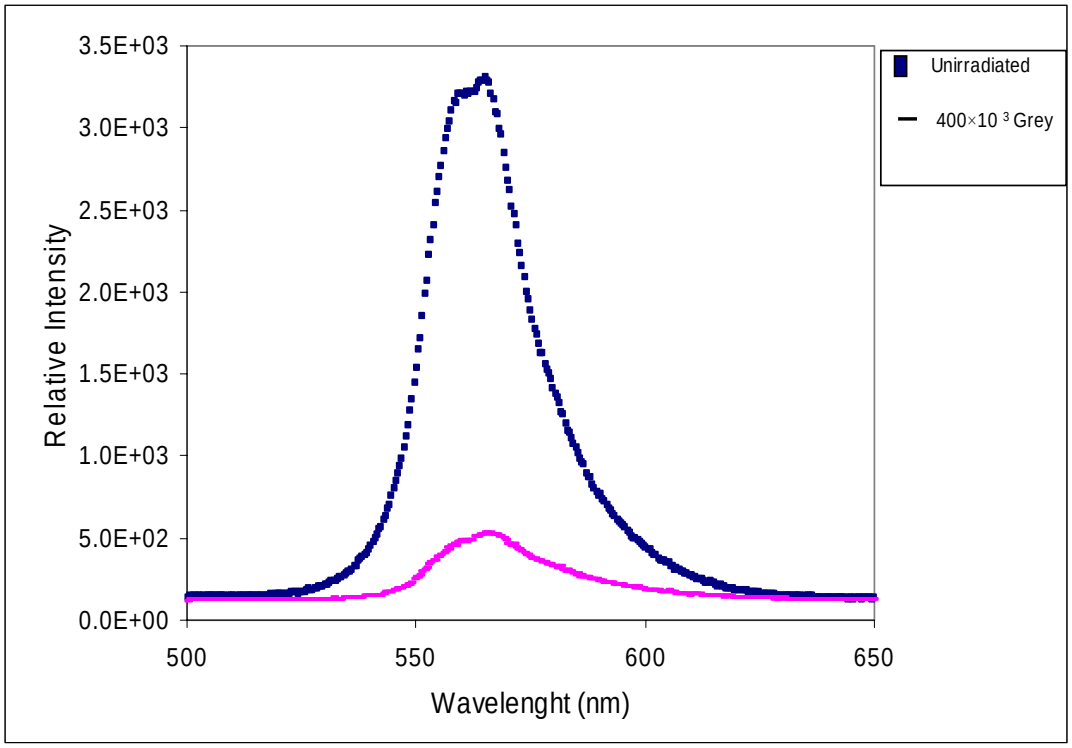

Figure10. Relative intensity as a function of wavelength of LED with a part number XLUG53D (green) before and after irradiation.

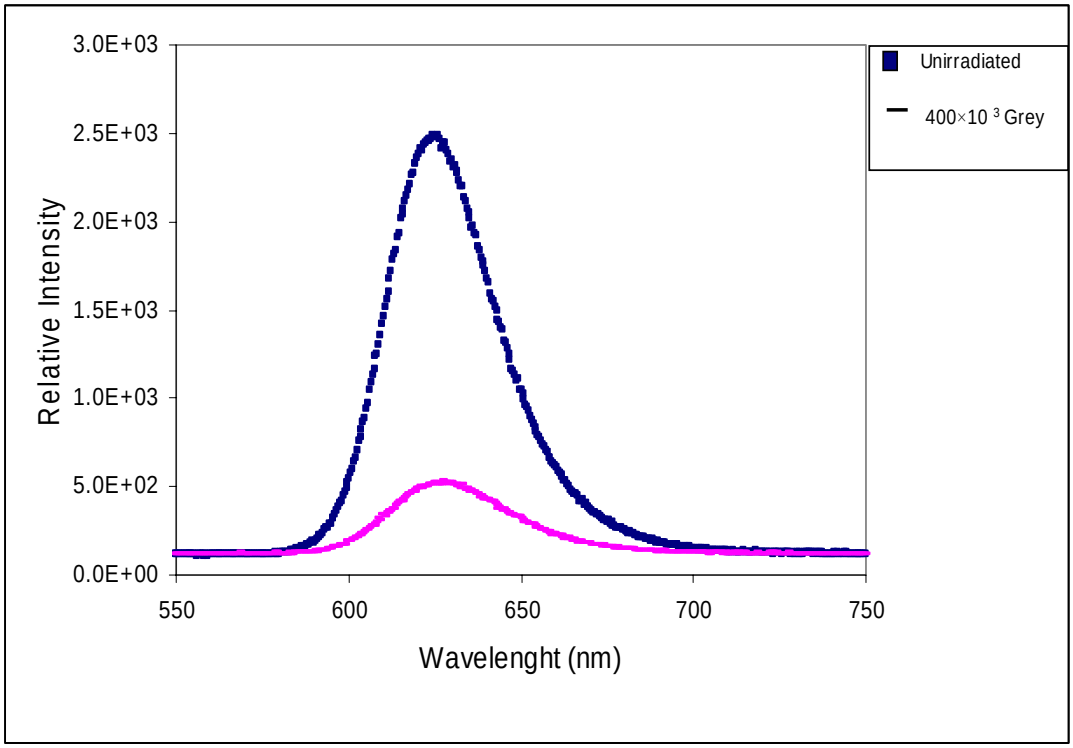

Figure 11 Relative intensity as a function of wavelength of LED with a part number XLUR53D (red) before and after irradiation.

CHAPTER 6

RESULTS AND DISCUSSION

Following gamma irradiation from a 60CO source to a total absorbed dose of 400×103 Grey, an increase in current (see Figures 5 and 6), and a reduction of electroluminescent spectral intensity is observed (see Figures 10 and 11) for green and red LEDs respectively.

We wish to further analyze the data in order to provide a basis for well understanding the changes upon irradiation. The method used in this study is based on the method proposed by Onoda et al, 2001 and Share et al, 1975 to analyze I-V characteristics. As observed from the Figures given for I-V characteristics, the current increases slightly. Definition of current given by Equation (4.73) provides to fit the data in order to find ideality factor given by n.

The semi log plot of current versus voltage is given by Figures 12 and 13. As explained in Chapter 4 Section (4.8), the recombination current dominates when ideality factor is 2 and recombination current dominates when the ideality factor is unity. This information will help us to understand the dominant current mechanism before and after irradiation.

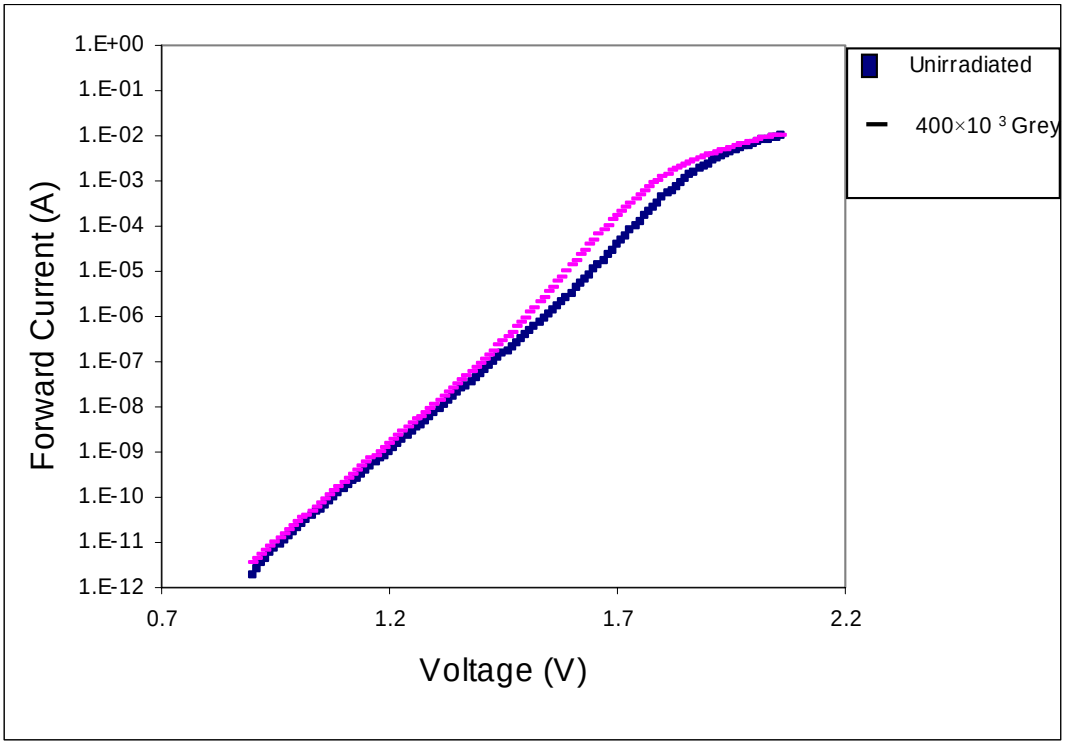

Figure 12. Typical current-voltage characteristics of LED with a part number XLUG53D (green) before and after irradiation.

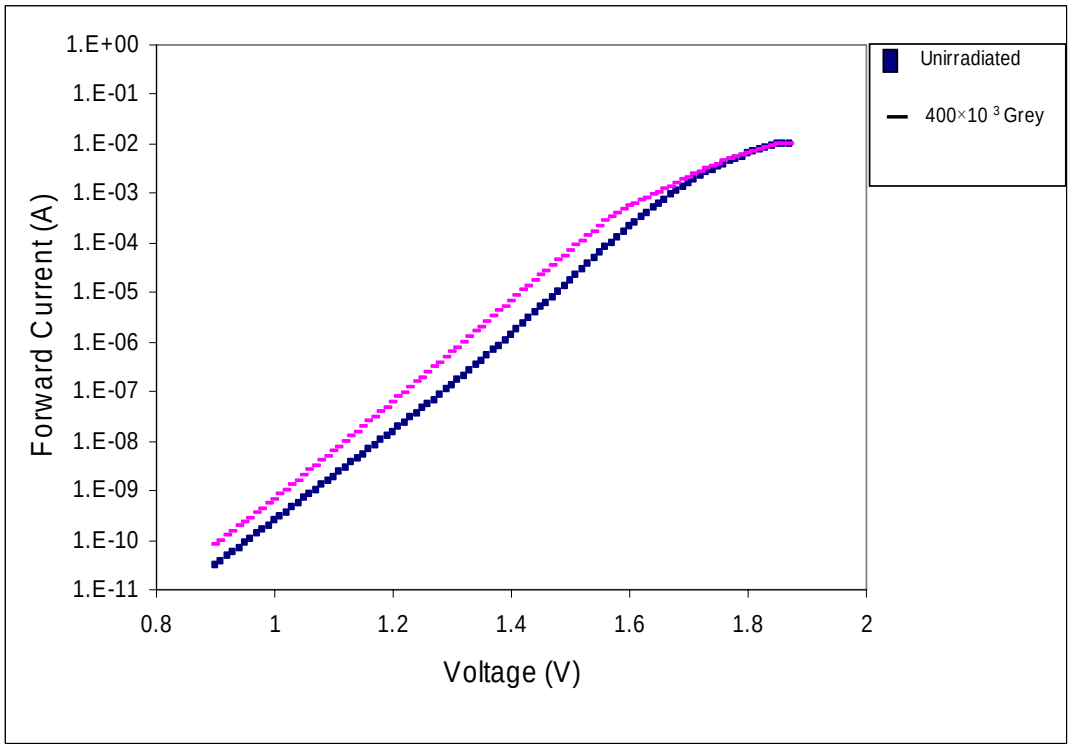

Figure 13. Typical current-voltage characteristics of LED with a part number XLUR53D (red) before and after irradiation.

6.1. I-V Studies and Current Transport Mechanism

As seen from Figure 12 (for green LED) for 1.5-1.85 V forward current increases with increasing total dose. In addition, the forward current is independent of dose up to around 1.5 V.

The tailing of the forward current at higher voltages is due to the series resistance. The ideality factor for green LED for unirradiated case is found to be around 2. After irradiation it is hard to define the slope with a single line. Therefore the line is analyzed in two voltage intervals; 0.9-1.5 V and 1.5-1.85 V. For the 0.9-1.5 V interval the ideality factor is constant and remains same as the unirradiated case and found to be 2.

For the voltages ranging from 1.5 to 1.85 the ideality factor decreases and becomes 1.54. For the fact explained in the previous section for the unirradiated case the current is dominated by the recombination current. After irradiation, it is observed that recombination current is dominant up to 1.5 V and, both recombination and diffusion currents are comparable in the voltage range of 1.5 -1.85 V.

Since in the voltage range 1.5 to 1.85 V the current is due to both recombination and diffusion, increase in current can not be defined whether it is due to increase in recombination or increase in diffusion current. To overcome this problem, we used Equation (4.62) which can be reduced to a second order polynomial with variable $\exp(\frac{qV}{2kT})$ and with zero intercept. Plotting current versus $\exp(\frac{qV}{2kT})$ and fitting the curve a second order polynomial gives us no significant change for the recombination current, implying that the increase in current is due to diffusion current.

A support to this interpretation has been discussed in (Share et al, 1975; Epstein et al, 1972) in which they have analyzed the light intensity versus voltage for GaAs and GaAsP LEDs. From the relation,

$$L = L_0 \exp(\frac{qV}{nkT}) . \tag{6.1}$$

They found that n is nearly 1 and it is constant with irradiation. The fact that the slope has a value of $n \approx 1$ radiative recombination occurs in the diffusion region of the diode. It was further reported that L_0 is a function of lifetime in the diffusion region of the diode (Onoda et al, 2001; Share et al, 1973; Gershenzon, 1966).
A further evidence is given by Epstein the value of the recombination current is inversely proportional to the lifetime in the space charge region of the diode. I0 is only slightly changed with irradiation and annealing suggesting that the lifetime in space charge region is not changing (Epstein et al, 1972).

Since the change is only in diffusion current, the radiation dependency of diffusion component is given by same as Equation (4.98) and repeated here as;

$$I_F = I_{D0}\sqrt{1 + K_p \tau_{p0} \Phi}\exp\left(\frac{qV}{kT}\right). \tag{6.2}$$

For the following analysis the increase in current will assumed to be due to increase in diffusion current.

To find the damage coefficient given by Equation (6.2) symbolized as $K_p \tau_{p0}$, at a given voltage the corresponding current values are chosen at all total doses given in the Section (5.1).This single voltage value is chosen as 1.7 V such that the current mechanism is assumed to be dominated by also diffusion and recombination currents and I_F is not affected by series resistance at this voltage.

The total dose dependence of the relative forward current at a bias 1.7 V after gamma irradiation is shown in Figure 14. Note calculations are corrected by taking the initial current values of each LED into account.

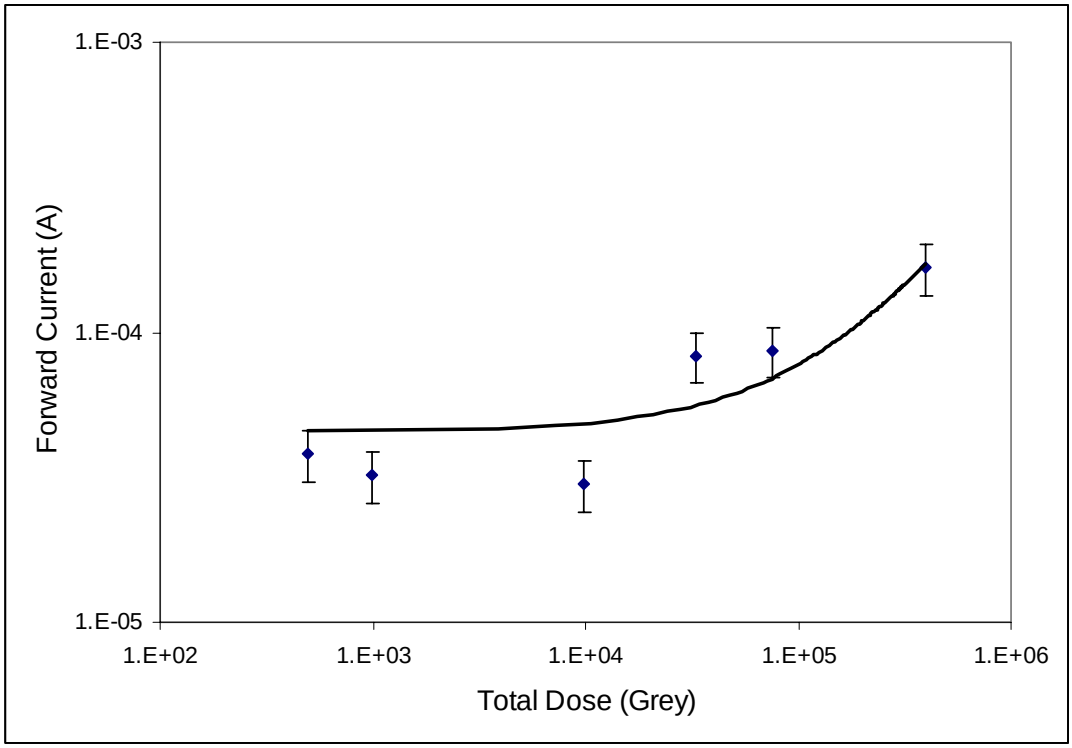

Figure 14. The total dose dependence of the forward current at a bias 1.7V of LED with a part number XLUG53D (green) irradiated with gamma rays.

From Figure 14 it is seen that current increases with the total dose. Increase in current will be analyzed through Equation (6.2). To analyze the increase in diffusion current separately, and from the fact that there is no information about the initial value of diffusion current, I_{D0} will be considered as an unknown coefficient. The experimental I_F is fitted to Equation (6.3) as a function of total dose. Since the current is fully dominated by recombination before radiation and it is also assumed to remain constant with the applied total doses, the diffusion currents will be found by subtracting the recombination current from the forward current. Subtracting forward current before irradiation at the given bias (1.7 V) from the currents after irradiation Equation (4.64) turns into

$$I_F - \frac{qW}{2} A\sigma v_{th} N_t n_i e^{qV_A/2kT} = q\left(\sqrt{\frac{D_p}{\tau_p}}\frac{n_i^2}{N_D}\right)A(e^{qV_A/kT}), \qquad (6.3)$$

the right side of this equation is diffusion current. With the minority carrier decrease

due to irradiation and combining Equation (6.3) with Equation (6.2) we have

$$I_F - \frac{qW}{2} A\sigma v_{th} N_t n_i e^{qV_A/2kT} = I_{D0}\sqrt{1 + K_p \tau_{p0} \Phi}\, \exp\left(\frac{qV}{kT}\right), \tag{6.4}$$

by taking the square of each side of the Equation (6.4) and dividing the each side by $\exp\left(\frac{qV}{kT}\right)$ term a linear equation can be derived as;

$$\left[\frac{I_F - \frac{qW}{2} A\sigma v_{th} n_i e^{qV_A/2kT}}{\exp\left(\frac{qV}{kT}\right)}\right]^2 = I_{D0}^2 + I_{D0}^2 K_p \tau_{p0} \Phi\,. \tag{6.5}$$

Equation (6.5) is used for fitting experimental values in order to obtain damage coefficient. From the intercept and the slope of the fitting curve the damage coefficient is estimated to be 1.3×10-4 (Grey)-1 for green LED.

The increase of the forward current after irradiation has been attributed in literature due to formation of defects. Onoda et al, 2001 has interpreted this due to decrease in minority carrier lifetime.

Furthermore; Epstein et al, 1972 have also reported that the irradiation introduces defects which decrease the lifetime. He also observed that annealing can be used to remove these defects to re-increase the lifetime.

The constancy of the recombination current with irradiation implies that the defect is either not located in the space charge region and/or is a shallow level located through the junction. A deep level in space charge region could act as an efficient recombination center causing an increase in the recombination current (Sze, 1969). If it is assumed that the defects are introduced throughout the junction, the defect energy level is shallow. Shallow defects introduced by irradiation have been observed in GaAs (Aukerman and Graft, 1962).

For the red LED different from the green one, the ideality factor is 1.84 before

irradiation and it remains constant after exposure of gamma irradiation. Since the error in the ideality factor is found as ± 0.10, the current mechanism is dominated by the recombination current can be assumed before and after the exposure. The effect of gamma irradiation to red LED is to shift the forward I-V characteristic to lower voltages without any noticeable change in the slope. Since the slope of the I-V curve given for red LED in Figure 13 is constant up to series resistance effects with the applied doses, change in current mechanism can not be analyzed as it was made for the green LED. Tunneling should explain the constancy of the I-V slope here, instead of increase found by others Epstein, Share and Barnes after exposure to gamma irradiation (Kushelevsky et al, 1983, Epstein et al, 1976). Lifetime decrease implies an increase of the product of $N_t\sigma$ where N_t is trap concentration and σ is recombination cross section. The recombination rate increase implies that the Fermi levels E_{FN} and E_{FP} are brought closer together as a result of irradiation. As $N_t\sigma$ increases with the increasing gamma doses the recombination current density given with Equation (4.60) increases. In order to find the damage constant in red LED, the increase in current will assumed to be effected due to the increase in recombination current. Combining Equations (4.61) and (4.92) and using the fact $N_t\sigma$ increases with the applied dose the effect of gamma exposure to the recombination current density can be written as;

$$J_{rec} = \frac{qW}{2}\sigma v_{th} N_t n_i \exp\left(\frac{qV_A}{2kT}\right) + \frac{qW}{2}\sigma v_{th} B\Phi n_i \exp\left(\frac{qV_A}{2kT}\right). \qquad (6.6)$$

A single voltage value and corresponding current values are chosen such that the current mechanism is not affected by the series resistance at this bias. The total dose dependence of the relative forward current at a bias 1.4 V after gamma irradiation is shown in Figure 15.

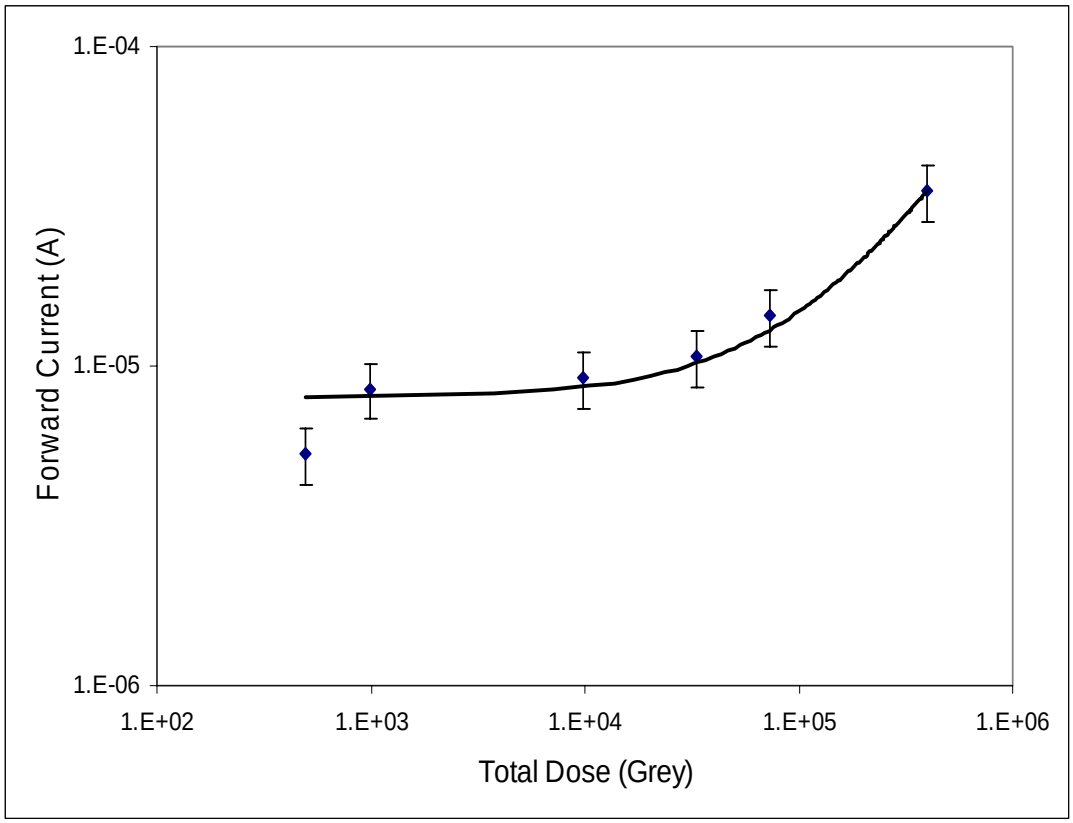

Figure 15. The total dose dependence of the forward current at a bias 1.7V of LED with a part number XLUR53D (Red) irradiated with gamma rays.

At a first approximation assuming that B is constant (Chaffin,1973) Equation (6.6) is used for fitting experimental values and B is estimated to be $8.75x10^{-6} N_t \left(\frac{1}{cm^3 Grey} \right)$. Further experimental analysis is required to understand the behavior of the dependence of the introduced defects on Φ.

In order to find the series resistance effect, knowing that the tailing is due to series resistance, I-V characteristics above 1.85 V (in Figure 12) are used. I-V characteristic above 1.85 V is re-plotted in Figure 16 for green LED.

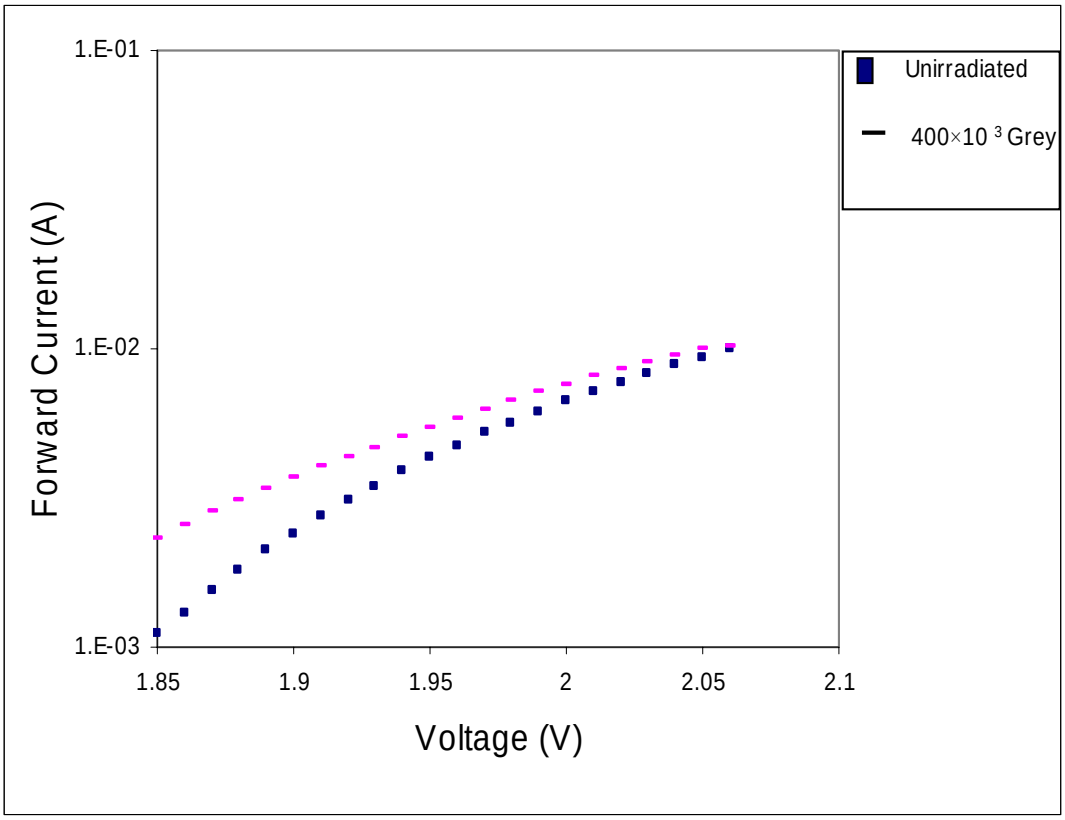

Figure 16. Typical current-voltage characteristics of LED with a part number XLUG53D (green) before and after irradiation.

Using Equation (4.67) for fitting the data gives the series resistance 13.66 Ω before irradiation and 13.10 Ω after irradiation for green LED. The tailing starts at 1.64 for the red LED as seen from Figure 13. With the same procedure, the series resistance is 10.37Ω before radiation and 9.99Ω after irradiation.

The error in series resistance is calculated to be ±0.20 Ω, so the change in series resistance is in the tolerance range and can be neglected. Series resistance is expected to increase with the exposure due to the degradation of mobility and carrier removal rate. The series resistance unaffected for the gamma doses up to 400x103 Grey.

It is well known that as a result of semiconductor irradiation with ionizing radiation many changes in bonding arise. Traps are generated and previously existing traps are neutralized. Gamma irradiation may have an overall effect of decreasing the proportion of deep traps and increasing the proportion of shallow traps, or doping impurities at the surface. (Kopeika et al, 1984).

6.2. C-V Characterization

Capacitance versus voltage graph for green LED is given by Figure 7. The capacitance-voltage characteristics of the diode is unaffected by the radiation up to doses tested. The experimental dependence of capacitance on voltage is given by Equation (4.76). Inverse-cube dependence of capacitance versus voltage resulting in a straight line for both types of diodes indicated that the junction is linearly graded. Typical C-V curves taken at a frequency of 1MHz for the LEDs XLUG53D and XLUR53D are shown in Figures 17 and 18.

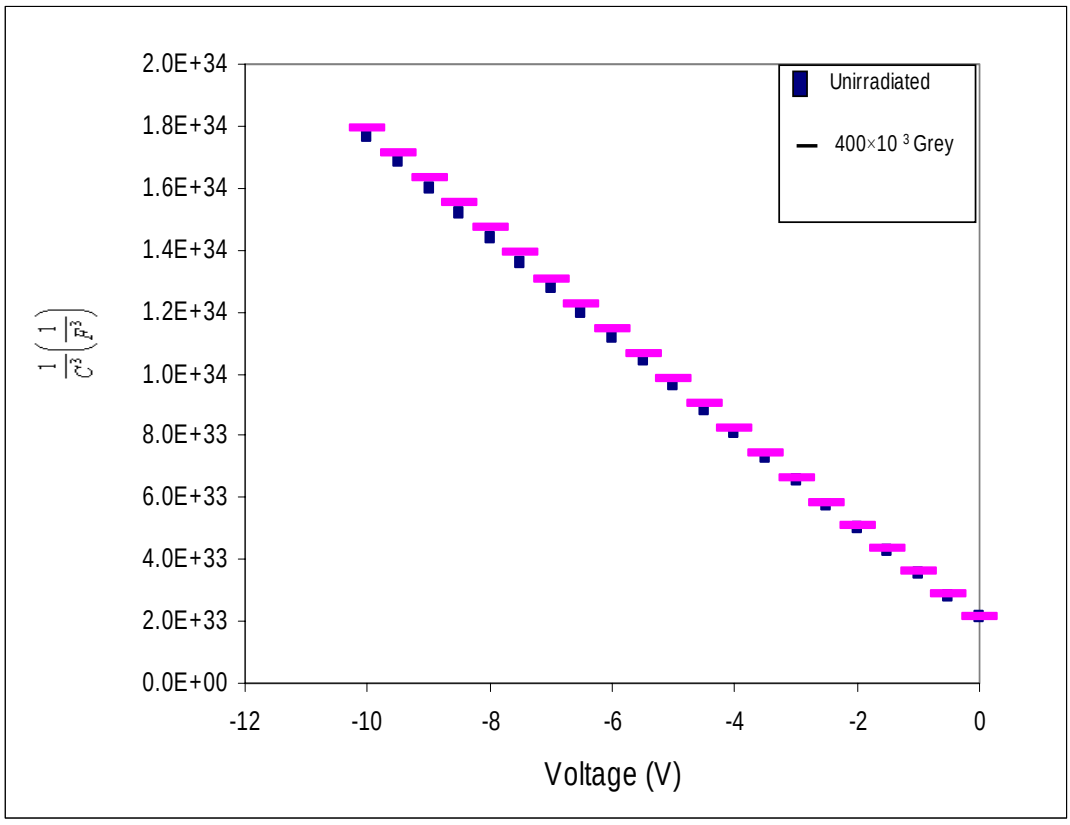

Figure 17. Inverse capacitance cubed versus voltage of LED with a part number XLUG53D (green) irradiated with gamma rays.

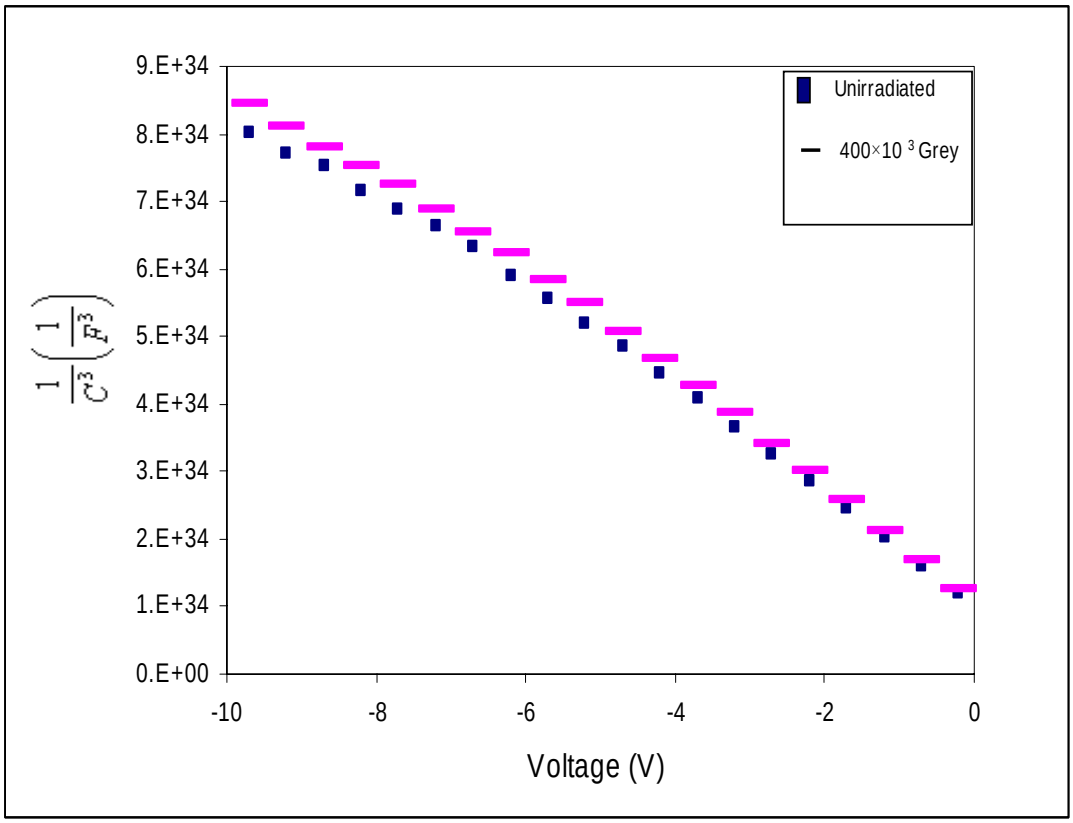

Figure 18. Inverse capacitance cubed versus voltage of LED with a part number XLUR53D (red) irradiated with gamma rays.

From Figure 16 the impurity distribution found by the slope remains constant with the applied dose. Since breakdown in these LEDs are nearly -10V it was not possible to probe deeper to p region. The depletion region is only a small fraction of the p region, the change or lack of change of the impurity distribution can not be determined by examining C-V characteristics for the green LED. Different from the green one in the red LED the slope of the inverse capacitance cubed versus voltage given with the Figure 18 changes and the change in the slope is out of the error range that can be considered as an increase in the impurity distribution in the depletion region of the LED.

A model to explain the increase in impurity density in GaAsP LED is proposed by Kopeika et al, 1983. According to them nuclear radiation can both produce new gap states and reduce the number or of gap states. This is so because the radiation can Displace atoms from their normal lattice positions thus forming vacancy and

interstitial atom
Fill vacancies, these in turn will rapidly form more complex lattice defects which behave much like impurities.

6.3. Spectral Response Analysis

Following gamma irradiation from 60Co source to a total absorbed dose 400×103 Grey, a reduction in the electroluminescent spectral intensity is observed as depicted in Figures 5 and 6. Before irradiation the GaP (green) LED has a spectral emission peak at 565 nm and a shoulder at 560 nm. After irradiation these values change as 565 nm and 559 nm respectively. The GaAsP (red) LED has a spectral emission peak at 624 nm before irradiation and it shifts to 627 nm after irradiation.

The peak emission wavelength remains constant for green LED as depicted in Figure 10. This result is consistent found by others (Epstein et al, 1972). A shift to longer wavelength is observed in red LED spectrum because of the constancy of I-V forward slope if the error in wavelength is taken to be 1 nm (given as the optical resolution of the spectrometer). It must be noted that, if the error is assumed to be 7 nm as calculated from the average of the repeated measurements, the change in peak emission wavelength can not be considered as a shift.

The decrease in peak spectral intensity can be explained by change in carrier lifetime and darkening of the encapsulation of the LED. In order to differentiate the effect of the darkening of the encapsulation due to irradiation, a constant light source is used and the percentage of the light passing through the encapsulation is found before and after irradiation. For the green LED the percentage of the constant light source passing through the encapsulation is 67.5 % and the percentage of the peak spectral intensity before and after radiation is 13 %. For the red LED these ratios are 51 % and 14 %. So it is seen that the decrease in peak spectral intensity due to darkening of the encapsulation and decrease in carrier lifetime. Another possible mechanism explaining the relative intensity drop is poisoning. The luminescent yield is decreased if the crystal is damaged by high energy radiation (which may be gamma rays or MeV range electron radiation). The incoming photon is absorbed by one molecule in the crystal; it stays there and is reemitted as luminescence. On the other

hand, if the molecule is damaged by radiation, then luminescence does not take place and the photon's energy is instead dissipated in the form of heat. All the molecules within a radius R of a damaged molecule are somehow poisoned, so that all molecules within that radius R, and not only the single molecule that is actually damaged, are unable to luminescence (Rosenstock and Schulman; 1968).

CHAPTER 7

CONCLUSIONS

In this study various aspects of radiation damage in light emitting diodes are investigated. Two types of LEDs are used in this study. We have performed gamma irradiation at various doses to GaP and GaAsP LEDs and measured I-V, C-V characteristics and spectral responses. Irradiation of GaP and GaAsP light emitting diodes in a 60Co source up to a dose of 400×103 Grey has resulted decrease in electroluminescent intensity and increase in forward current. No noticeable change is observed in the series resistances up to total doses tested. The impurity density which can be deduced from the C-V measurement remains same in the green LED and increases in the red one due to the irradiation.

A detailed analysis of the current transport mechanism in light emitting diodes has shown that the forward current is dominated by the recombination current component before the exposure. In green LED after the exposure, diffusion contribution to the forward current starts to dominate. This can be explained by a decrease in the minority carrier lifetime. Different from the green LED (GaP), in the red one (GaAsP) the current transport mechanism type is not affected noticeably with the exposure. For the red one increase in current is attributed to the tunneling, due to the slight increase in impurity concentration caused by the radiation.

Different conclusions can be drawn when the changes in the properties of GaP and GaAsP LEDs due to irradiation are compared. For the green one, the damage mechanism can be explained that the produced defects are not located in the space charge region and/or the defects are shallow. In the red LED the trap density increases with the exposure causing an increase in the recombination current.

Damage coefficient for the green one is estimated to be 1.3×10-4 (Grey)-1 and the term B which is related to the trap density (as given in (Chaffin, R. J., 1973)) for the

red one is estimated to be $8.75x10^{-6} N_t \left(\frac{1}{cm^3 Grey} \right)$. Since this term is a function of the trap density, it was assumed to be constant in the calculations due to lack of more detailed experimental data. For the derivation of the dependency of the trap density on the total applied dose, additional experiments determining the trap densities independently before and after the exposure should be performed. However, since in this work experiments were performed on commercial devices and we could not obtain the materials in the bulk form to carry out the further work.

The relative intensity reduction for both types of devices, after the exposure was attributed to darkening of the encapsulations and also to the formation of defects which decrease the minority carrier life time (Onada et al, 2001; Epstein et al, 1972). Furthermore, dissipation of energy in the form of heat due to damaged molecules might also be another cause of the intensity reduction due to irradiation (poisoning (Rosenstock and Schulman; 1968)).

The constancy of the peak wavelength in GaP LED may be explained with the formation of defects in the space charge region or the shallowness of the defects if located in the junction region. Shift to longer wavelengths in GaAsP LED was attributed to constancy of I-V forward slope in the literature which decreases the energy difference between E_i in the surface and the bulk (Kushelevsky et al, 1983).
In order to expand the research, additional experiments should be performed such as Hall Effect measurements that give information about mobility, resistivity and carrier density of the bulk material. It also yields the scattering mechanisms when performed as a function of temperature. In addition to these studies, the energy and the densities of the trap levels can be measured to support experimentally the constancy of recombination current in GaP LED. As given in section 6.2, the radiation can form lattice defects. To cure these defects optimal annealing temperature and duration can also be investigated
As the technologies for LED production are developing rapidly, the samples used in this research can be diversified. This variation through the samples can lead to find much more robust device in the radiation environment.

At the end the conclusion can be drawn as, due to small changes of the measured quantities of the light emitting diodes, they are robust under the exposure and they do not cause significant operational failures.

REFERANCES

Aukerman, L. W., and Graft, R. D., *Phys. Rev*., **127**, 1576-1583, 1962.

Barnes, C. E.*, J. Appl. Phys*., **42**, 1941-1949, 1971.

Barnes, C. E., *Journal of Applied Physics*, **50**, 5242-5250, 1979.

Blakemore, J.S., *Semiconductor Statistics*, Pergamon Press, New York, 1962.

Chaffin, R. J., *Microwave Semiconductor Devices: Fundamentals and Radiation Effects*, A Wiley Interscience Publication John Wiley & Sons, London, 1973.

Corbett, J.W., *Electron Radiation Damage in Semiconductors and Metals*, Academic Press, New York, 1966.

Epstein, A. S., Share, S., Polimadei, R. A., Herzog, A. H., *IEEE Trans. Nucl. Sci*., **19**, 386-390, 1972.

Epstein, A. S., Share, S., Polimadei, R. A., *IEEE Trans. Nucl. Sci*. **23**, 1654-1663, 1976.

Evans, R. D., *The Atomic Nucleus*, McGraw Hill, UK, 1955.

Gershenzon, M., Logan, R.A., Nelson, D.F., *Phys. Rev*., **149**, 580-597, 1966.

Hirsh, I.; Hava, S.; Kopeika, N.; Kushelevsky, A.; Alfassi, Z.; Aharoni, H.; Polak, M., *IEEE Journal of Quantum Electronics*, 19, 29-33, 1983.

Kopeika, N. S., Hava, S., Hirsh, I., *IEEE Journal of Quantum Electronics*, 20, 63-71, 1984.

Landsberg, P.T., Beattie, A. R., *Phys. Chem. Solids*, **8**, 73-75, 1959.

Lax, M., *Physics and Chemistry of Solids*, **8**, 66-73, 1959.

Leo, W.R., *Techniques for Nuclear and Particle Physics Experiments*, 2nd Revised edition, Springer-Verlag, 1994.

Onoda, S., Mori, H., Okamoto, T., Hirao, T., Itoh, H., Okada, S., *Rad. Phys. and Chem.*, **60**, 377-380, 2001.

Rosenstock, H. B., Schulman, J. H., *Localized excitations in solids*, Plenum Press,

New York, 1968.

Schubert E. F., *Light Emitting Diodes*, Cambridge University Press, USA, 2003.

Share, S., Epstein, A. S., Polimadei, R.A.., *Solid-State Electronics*, **18**, 471-480, 1975.

Share, S., Epstein, A. S., Polimadei, R., A., *IEEE Trans. Nucl. Sci.,* **20**, 256-260, 1973.

Spinks, J. W. T. and Woods, R. J., *An Introduction to Radiation Chemistry*, John Wiley and Sons, London, 1964.

Sze, S. M., *Physics of semiconductor devices*, Wiley-Interscience, New York, 1969.

Tyagi, M., S., *Introduction to semiconductor Materials and Devices*, Jonh Wiley and Sons, London, 1934.

Watkins,G.D., *ERP and Optical Absorption Studies in Irradiated Semiconductors, Radiation Effects in Semiconductors,* Plenum Press , New York, 1968.

Woolf, S. and Frederickson, A. R., *IEEE Transactions on Nuclear Science*. **6**, 4371-4376, 1983.